Spectrocolorimetric interpretation of sedimentary dynamics: The new "Q7/4 diagram"

Maxime Debret, D. Sebag, Marc Desmet, W. Balsam, Y. Copard, B. Mourier, A.S. Susperrigui, Fabien Arnaud, I. Bentaleb, Emmanuel Chapron, et al.

HAL Id: insu-00615505

https://hal-insu.archives-ouvertes.fr/insu-00615505

Submitted on 10 Oct 2011

Spectrocolorimetric interpretation of sedimentary dynamics: The new "Q7/4 diagram"

Debret, M. [1,2], Sebag, D. [1], Desmet, M. [2,3], Balsam, W. [4], Copard [1], Y., Mourier, B. [5], Susperrigui, A.-S. [6,7], Arnaud, F. [8], Bentaleb, I. [9], Chapron, E. [2], Lalliers-Vergès, E. [2], Winiarski, T.[3]

[1] *Laboratoire de Morphodynamique Continentale et Côtière, Université de Rouen, UMR CNRS 6143, 76821 Mont-Saint-Aignan, France, Université de Caen,* UMR CNRS 6143, 14 000 Caen, France.

[2] *Institut des Sciences de la Terre d'Orléans, Université d'Orléans et Université François Rabelais de Tours, UMR CNRS 6113, 45071 Orléans Cedex 2, France.*

[3] *Laboratoire des Sciences de l'Environnement, Ecole Nationale des Travaux Publics de l'Etat, 69518 Vaulx-en-Velin Cedex, France.*

[4] *Department of Earth and Environmental Sciences, University of Texas at Arlington, Arlington, TX, USA*

[5] *Laboratoire Chrono-Environnement, Université de Franche Comté, UMR 6249 Place Leclerc F-25030 Besançon Cedex, France.*

[6] *Departement genie civil, équipe matériaux, Insa Rennes, 20 avenue des Buttes de Coësmes, 35708 Rennes Cedex 7, France.*

[7] *Laboratoire d'étude des Transferts en Hydrologie et Environnement, Université Joseph Fourier, UMR 5564 (CNRS, INPG, IRD, UJF), BP 53, 38041-Grenoble Cedex 9, France.*

[9] *Institut Méditerranée d'Ecologie et de Paléoécologie, UMR CNRS 6116, Europôle de l'Arbois, 13454 Aix-en-Provence cedex 04.*

[10] *Laboratoire des Environnements, DYnamiques, TErritoires de la Montagne, Université de Savoie, UMR CNRS 5204, 73376 Le Bourget du Lac, France.*

[11] *Laboratoire de Géodynamique des Chaînes Alpines, Université de Savoie, UMR CNRS 5025, 73376 Le Bourget du Lac, France.*

Abstract

Colour is a fundamental property of sediment and is often used for lithographic description to determine sedimentological structures, facies etc. However, the information contained in this parameter is difficult to extract because it is difficult to quantify. Colour can be quantified by spectrocolorimetry which provides very high resolution data quickly and non-destructively. When adapted to sedimentology, spectrocolorimeters prove to be powerful tools due to their low purchase and maintenance costs, and some are portable and easily used in-the-field. Several methods have been used to extract sedimentological data from colorimetric spectra (first derivatives, factorial analysis, etc.). In the present study, we first provide a review of the sedimentological application of spectrophotometers and, after having described these methods, their advantages and disadvantages, we then describe a new tool called the Q7/4 diagram (abscissa L*; Ordinates 700/400 ratio). This new technique permits sedimentological units to be defined, allows the identification of different sediment components and provides 5 distinct poles: Clayey deposits, organic rich deposits (chlorophyll a and by products), altered organic matter deposits, iron rich deposits, carbonated deposits. Coupled with the analysis of first derivative spectra, it is possible to distinguish different pigments linked to the

degradation and/or nature of the organic material (Chlorophyll a, melanoidin, etc.), the state of iron oxidation (for example, hematite and goethite-like signatures) and the nature of clays. The Q7/4 diagram permits rapid acquisition of high resolution data on changes of sediment dynamics in geosystems that have been subjected to highly varied climatic/environmental conditions. The instrument is non destructive, easy to use and maintain, portable for use in the field, fast to implement, is capable of high resolution, and has a vast range of possible applications. Spectrocolorimetry appears to provide many advantages and could become an essential and robust tool for preliminary sedimentological studies.

Keywords: Spectrophotometry, Reflectance, Q7/4 diagram, First derivative spectra, Lake, Fjord, Peat, Organic matter, Chlorophyll a, Iron, Carbonate, clay.

1. Introduction

A key focus of modern sedimentology is to develop new analytical approaches providing high resolution paleoclimatic/paleoenvironmental data (i.e. continuous signals and short-time fluctuations). The many approaches based on geochemical analyses provide a variety of sensitive proxies (e.g. mineralogy, elemental or isotopic composition) from different sedimentary records (carbonate, silicate or organic fractions of sediments). Thus, sedimentologists use geochemical proxies to reconstruct paleoenvironments and climate dynamics.

However, most of these analyses require destructive laboratory procedures that produce a description of continuous events (i.e. sedimentary, climate or landscape dynamics) from intermittent measurements (i.e. analyzed samples). The intermittent nature of the sample can be ameliorated by reducing the sampling interval, but this can greatly multiply the number of measurements needed. Some techniques (e.g. XRF core scanner, diagraphy, tomography)

have allowed for the acquisition of continuous data from sedimentary records (i.e. drilling, cores, sections), but they often require specific equipment and turn out to be complex and very expensive. As a result, alternative solutions have been proposed, such as digitized image analysis (e.g. Tiljander et al, 2002) and grey scale analyses (Boes et al, 2005). However, grey-level analysis is restrictive in that it only distinguishes between mixtures of white (i.e. quartz and carbonated fractions) and dark components (i.e. clayey and organic fractions).

Nevertheless, sediment colour has always been considered an important qualitative parameter, used to describe and distinguish sedimentary facies (e.g. Munsell chart) and related to mineralogical composition. Colour has also been used to describe marine and continental sediments, surficial deposits and soil horizons by using charts (i.e. reference scales), the best known of these being the Munsell colour classification. For example, the distribution of "brick red lutites" was initially performed by using the Geological Society of America Rock-Colour Chart (e.g. Ericson et al., 1961; Heezen et al., 1966; Hollister & Heezen, 1972), because the unique bright red colour of these sediments is a useful characteristic, aiding their identification and was later quantified by spectral methods (Barranco et al, 1989).

However, using colour as a scientific tool has well-known disadvantages, as this approach is subjective and depends on numerous parameters such as lighting, sediment texture (matt or shiny), the colour of the background, the size of the object, the type of illumination, etc. The most serious disadvantage is the non-quantitative nature of colour determination. Thus, it is necessary to develop objective methods based on precise and reproducible measurements. That is why the development of an industrial device for accurately quantifying colour has attracted the attention of researchers, and this kind of device is now in use. It is easy to operate and increasingly used in routine operations to objectively characterize deposits and sedimentary facies (e.g. Curry et al, 1995; Mix et al, 1992; Balsam et al 1997). However, its scientific implementation is too often limited to measuring reflectance, which corresponds to

the indirect measurement of a greyscale (e.g. Chapmann and Shackleton, 1998). Nevertheless, several more detailed studies have shown that these measurements can be used to identify the mineralogical composition of sediments, especially in marine environments. For example, during various Ocean Drilling Program (ODP) legs aboard the JOIDES Resolution (and aboard Marion Dufresne RV for the IMAGE program), optical lightness (L*) data are commonly used to correlate between cores in order to determine glacial–interglacial climatic cycles and down-core changes in mineral composition (e.g., Mix et al., 1992, 1995; Schneider et al., 1995; Balsam et al., 1997, 1998, 1999; Weber, 1998; Balsam and Damuth 2000; Giosan et al., 2001, Balsam and Beeson, 2003, Debret et al, 2006).

This paper examines the sedimentological potential of spectrophotometric analysis as an environmental proxy. We shall show, through a comparative analysis of previously published studies and new results, how the "Q7/4 ratio" can be used in a "Q7/4 *vs·* L* diagram" to characterize marine and continental sediments (i.e. calcareous, clastic and organic facies) and supply qualitative and\or quantitative information. We then discuss spectral signatures that are related to sedimentary dynamics.

2. Diffuse Visible Reflectance: common uses in sedimentology

Colour is the human eye's perception of reflected radiation in the visible region of the electromagnetic spectrum (400–700 nm). One of the most objective ways to measure colour is through the use of diffuse-reflectance spectrophotometry. Light reflected from a material is collected in an integrating sphere and normalized to the illuminant, the light source. Instruments are calibrated by setting the 100% reflection level with a pure white standard (frequently barium sulphate) and the 0% reflection in a light-free box. Calibration is done over the entire wavelength range of the visible light spectrum. According to the CIE Lab method, tristimulus values (X, Y, Z) are derived from colour reflectance, then used to convert

measurements to one colour space, such as the Yxy, L*a*b* and its derivative L*C*H°, Lab, and L*u*v* systems.

In 1987, Deaton used a reflectance spectrophotometer to quantify rock colour from Munsell charts, however, where in the laboratory or where a portable spectrocolorimeter is available the L*a*b* system (Fig 1) has replaced the Munsell system for rock colour analyses. It is far superior to, and therefore has replaced, the Munsell colour system traditionally used in Earth Science. This approach was descriptive, but provides reproducible and objective measurements of rock colour. It opened the road for numerous new applications, especially for quantitative estimations and qualitative identifications of colour-bearing sedimentary constituents. However, the methods used varied from the direct use of common chromatic parameters to more specific processing of raw measurements. Here, we present only their outlines with a few examples of application.

2.1. Standard parameters: the L*a*b* system

The standard chromatic parameters (*i.e.* coordinates in an R.V.B. colour space) are now commonly used to measure and compare the lightness and colour of samples in sedimentology and soil sciences (*e.g.* Sánchez-Marañón et al., 1997 and 2003; Kirby *et al.*, 1999; Piper & Hundert, 2002; Wang *et al.*, 2006; Cohen *et al.*, 2009; Guedes *et al.*, 2009; Magela da Costa *et al.*, 2009; Ortiz *et al.*, 2009; Martínez-Carreras *et al.*, 2010; Weber *et al.*, in press).

At the present time the L*a*b* system (Fig 1) is the most commonly used colour space in sedimentology and is also referred to as the CIELAB system. It can be visualized as a spherical coordinate system in which one of the axes of the sphere is the lightness variable L*, ranging from 0% to 100%, and the other axes are chromaticity variables a* and b*.

Variable a* is the green (negative) to red (positive) axis, and variable b* is the blue (negative) to yellow (positive) axis.

These standard parameters can often be used to provide detailed time series of relative changes in the composition of the bulk sediments and are frequently used to tune sections from core to core or hole to hole and to analyze the cyclicity of lithological changes. For example, Chapman & Shackleton (1998) used the L*a*b* parameters to establish precise centimetre-scale correlations between deep-sea cores (Gardar Drift, North Atlantic). Then, they concluded that small-scale variability marked by abrupt changes in lightness and colour provided a potentially meaningful century-scale sedimentary record.

The use of total reflectance (L* parameter) to measure sediment brightness is commonly used in sedimentology (*e.g.* Chapman & Shackleton, 1998; Bozzano *et al.*, 2002; Wilson & Austin, 2002; Jin *et al.*, 2005, Debret et al, 2010). For example, Balsam and Deaton (1991) employed a diffuse reflectance spectrophotometer to examine marine top-cores (North and South Atlantic) and noted a positive correlation between sample brightness and carbonate content (e.g. Mix et al, 1995 for ODP cruise). Later, Balsam *et al.* (1999) compared gray scale, brightness and L* to show that all measurements of optical lightness are reasonable proxies of relative but not absolute changes in carbonate content. In addition, this highlights that changes in the composition of the non-carbonate sediment fraction may significantly alter the relationship between lightness and carbonate content. Similarly, Roth & Reijmer (2005) used a correlation between XRD measurements and L* values to quantify and analyse the high-resolution fluctuations of aragonite content related to millennial paleoclimatic variability in marine sediments (Great Bahama Bank).

a* and b* parameters can also be used separately to track one or more sediment components. Because red-green was assumed to be related to red-coloured iron-bearing terrigenous

material, the green–red colour ratio (a* parameter) has sometimes been used to track changes

in ice-rafted inputs related to large-amplitude millennial-scale climate variability in the

Northeastern Atlantic (Rockall Plateau; Helmke *et al.*, 2002) and Pacific (West Antarctic

Peninsula; Hepp *et al.*, 2005). Likewise, the parameter b* was used by Debret *et al.*

(2006) as an indicator of diatom content closely linked with upwelling intensity in fjord

deposits (Saanich Inlet, Canada).

Thus applications based on standard parameters are routinely published for

paleoenvironmental and paleoclimatic reconstructions (*e.g.* Wolf-Welling *et al.*, 2001;

Wilson & Austin, 2002; Yu *et al.*, 2006; Dubois *et al.*, 2008). This use is particularly

suitable for sediments containing a mixture of two colour-contrasted constituents, such as a

white component (carbonate or quartz) and a darker one (clay or organic material). Once

calibrated with direct qualitative analysis (mineralogy, geochemistry, etc.), these parameters

may provide a continuous sedimentary signal and high-resolution measurement of changes in

sediment composition (Rothwell & Rack, 2006). However, these standard parameters do not

provide qualitative information. In addition, they produce only aggregate data for the

lightness and colour of the samples studied, while the raw measurements are performed by

wavelength.

2.2. Raw data: Visible Reflectance Spectra

The raw data measured by the device can be used to trace change in the visible reflectance

spectrum (VRS), representing the reflectance measured (%) as a function of wavelength (from

400 to 700 nm for the visible spectrum; Figure 1) relative to a standard. Each spectrum is

therefore characteristic of the colour and lightness of the sample studied. Although VIS

spectra are difficult to interpret, they have nonetheless been used (*e.g.* Deaton & Balsam,

1996; Wolf-Welling *et al*, 2001; Barrett, 2002; Rein & Sirocko, 2002; Sánchez-Marañón *et al*, 2007). For example, Balsam *et al* (1998) showed that VIS derived from wet cores are darker than those derived from dry samples and may contain less information about mineralogy and composition. In addition, in sediments whose water content is higher than about 5%, the decrease in reflectance is greater at the red end of the spectrum than at the violet end, thereby muting the spectral signal. By contrast, when sediment water content is less than 5%, VIS are somewhat darker than curves from dried sediment, but give a similar shape.

2.3. Reflectance in colour bands

The VIS can also be analysed for a band of wavelengths corresponding to a range of colours (violet = 400–450 nm, blue = 450–490 nm, green = 490–560 nm, yellow = 560–590 nm, orange = 590–630 nm, and red = 630–700 nm). Percent reflectance in each colour band can be calculated by dividing the percentage of reflectance in a colour band by the total reflectance in a sample (Mix et al, 1992, 1995). Thus Ellwood and Brooks (1995) used spectral reflectance in red colour range to track the changes in hematite content related to paleosoil surfaces in two excavation infillings (River Bend site, Trinity River floodplain, Texas). Similarly, Ji *et al* (2005) used redness (*i.e.* percent reflectance in the red colour band) to track high-resolution colour changes in lacustrine sediments (Qinghai Lake, northeastern Tibetan Plateau), suggesting periodicity in Asian paleomonsoon fluctuations.

Ji *et al's* (2005) work suggests that once calibrated with direct measurements, the variations for each colour range can be correlated with changes in one or more constituents of sediment: clay minerals, carbonate, opal, hematite, goethite, organic matter, glauconite, and/or phosphorite content, for example. In numerous studies, spectral violet, blue, green, yellow, orange, red, and brightness have been used as independent variables for multiple linear

regression or factorial analysis. Following comprehensive calibration, equations provide function-derived transfers that serve as valuable estimates of sediment composition, and as proxies for studying East Asian paleomosoon variability (Luochuan and Lingtai loess sections, central Chinese Loess Plateau; Ji *et al*, 2001; Balsam et al., 2004) and the co-evolution of paleomosoon and paleo-El Niño (South China Sea; Zhang *et al*, 2007), sources of fluvial sediment input (186 top cores samples distributed throughout the Gulf of Mexico; Balsam & Beeson, 2003), differences in composition of detrital input and diagenetic processes (western North Atlantic drifts; Giosan *et al*, 2002), and the geological and pedological processes in paleosoils (Peoria Loess, middle Mississippi River Valley; Wang *et al*, 2006). For example, Balsam & Deaton (1996) examined calibration tests for assessing compositional changes in Late Quaternary marine sediments (356 samples from various sites). They used multiple regression models calibrated on direct measurements to estimate carbonate content (Atlantic and East Pacific Rise), organic carbon content (Atlantic and East Pacific Rise), and opal content (East Pacific Rise). These tests indicated that transfer-equations reasonably estimate the pattern of changes, but frequently over or underestimate the values observed. Nevertheless, differences between the sites studied indicate that local conditions strongly influence spectra and as Ji *et al* (2004) indicated calibration equations based on spectra cannot be applied globally.

2.4. *Different indices*

Raw data can also be used to calculate ratios between two wavelength bands. Thus Bahr *et al* (2005) conducted a high-resolution multi-proxy study on cores from a continental slope

(NW Black Sea). In this study, they used a red/blue ratio, calculated as the ratio between the 700 nm and 450 nm wavelengths, to plot changes in sedimentary composition and colour.

Another approach consists in calculating different indices based on specific wavelengths. Recently, Kovalev & Nichiporovich (2003) proposed a new integral index based on four wavelengths (λ = 660, 700, 740, and 750 nm) that is more informative in comparison with that widely used in soil science and based on nine gradations.

Reflectance spectrophotometry has also been used to study organic components, especially pigments like chlorophyll and carotenoid (*e.g.* Lovelock & Robinson, 2002; Das *et al.*, 2005; Murphy *et al.*, 2005; Khan *et al.*, 2009; Von Gunten *et al.*, 2009). Thus Rein & Sirocko (2002) tested different ratios at distinct wavelength ranges and values (660–670, 600–610, 510, 460 and 410 nm) for quantitative pigment estimations in Quaternary marine cores.

Recently, Wolfe *et al.* (2006) demonstrated that ubiquitous troughs in sediment reflectance near 675 nm are attributable to chlorophyll a and derivative compounds. In addition, they obtained significant correlation between the area of the reflectance trough in the 650–700 nm interval and summed concentrations of chlorophyll a and by-products.

Finally, all VIS analyses show that certain ranges of colour are preferentially related to specific sedimentary components, for example, between 470 and 580 nm for iron oxides; between 400 and 470 nm and between 605 and 680 nm for clay minerals and carbonates, and between 650 and 700 nm for organic compounds. These observations highlight the possibility of using spectrophotometric measurements to both determine the nature of main components and qualitative changes in sediment composition.

2.5. First Derivative Spectra

Based on these observations, the First Derivative reflectance Spectra (FDS) method was proposed in order to determine sediment mineralogical composition with precision (Barranco

et al., 1989; Balsam & Deaton, 1991; Deaton & Balsam, 1991). Different studies have shown that some sedimentary components have distinctive spectral signatures identified by the position of first derivative peaks: 445 and 525 nm for iron oxyhydroxides such as goethite; 555, 565 and 575 nm iron oxides such as hematite; and from 605 to 695 nm for organic compounds, etc. (Fig 2).

The analysis of FDS to identify colour-key components is now well documented for marine, lacustrine (See Fig 2 for lake Le Bourget down core FDS), and fluvial sediments (*e.g.* Balsam & Deaton, 1996; Balsam *et al.*, 1998; Ortiz *et al.*, 1999; Helmke *et al.*, 2002; Balsam & Beeson, 2003; Horneman *et al.*, 2004; Debret *et al.*, 2006; Chapron *et al.*, 2007; Zhang *et al.*, 2007; Koptíková *et al.*, 2010; Michelutti *et al.*, 2010), for soils and terrestrial surficial deposits (*e.g.* Wang *et al.*, 2006; Miralles *et al.*, 2007; Zhou *et al.*, 2010), and for dust and aeolian deposits (Ji *et al.*, 2001 and 2005; Arimoto *et al.*, 2002; Shen *et al.*, 2006).

In order to test quantitative processing, Balsam & Deaton (1991) analyzed FDS and identified a factor that appeared to be related to carbonate content in 178 marine surface sediments (different sites in the Atlantic Ocean). However, the weak correlation coefficient suggests that this variable was controlled by additional components. Later, other authors used the same approach to track mineralogical changes in Neogene (ODP Leg 172, central Atlantic Ocean; Giosan *et al.*, 2001) and Holocene (Chukchi Sea, Alaskan margin; Ortiz *et al.*; 2009) marine deposits. FDS also de-emphasizes the importance of absolute percent reflectance values, thereby reducing the significance of slight differences in calibration (Damuth & Balsam, 2003). Nevertheless, this approach is limited by the mathematical derivative that

allows a qualitative assessment but no quantitative estimation of the abundance of different sediment components.

2.6. Interest and limitation: comparative synthesis

For binary mixtures of contrasted constituents (i.e. dark/light), the standard parameters of the CIELab reference have been used directly for paleoenvironmental and paleoclimatic purposes (e.g. Helmke et al., 2002; Roth & Reijmer, 2005; Debret et al., 2006). However, for most of the continental and marine deposits formed from complex mixtures, other parameters can be analysed and several types of approach have been proposed (e.g. Balsam & Beeson, 2003; Ji et al., 2005; Wolfe et al., 2006; Ortiz et al., 2009). A fairly general comparison of their advantages and limits (see Table) makes it possible to associate with each tool (i.e. VIS, colour bands, index, etc.) to a preferential field of application ranging from the characterisation of sedimentary facies (e.g. Balsam et al., 1997) to the quantitative estimation of certain constituents (e.g. Zhang et al., 2007) and, in certain specific cases, genuine quantification calibrated by chemical analysis (e.g. Damuth & Balsam, 2003). However, from a statistical standpoint, VIS and FDS exhibit a high degree of colinearity, making the choice of variables difficult. The initial choice of independent wavelengths to be included in an equation or index is complex and should be based on several types of preliminary analyses (including correlation matrices, factor analysis, and step-wise regression). However, as with the standard parameters (L*, a*, b*), the interpretation of measurements always requires a preliminary calibration from direct sedimentary qualitative analyses. Therefore this comprehensive approach provides equations that should be used with care to avoid non-analogue situations. In conclusion, VIS and FDS can be used with caution to track high-resolution fluctuations in sedimentary composition, particularly for binary mixtures of colour-contrasted constituents.

3. Spectrophotometry: methodology and Q7/4 diagram

3.1. Instrumentation

All the data presented in this paper were obtained by using the same instrument, namely a Minolta CM 2600d. The spectrocolorimeter is composed of a sphere; the surface of the sphere is coated with barium sulphate. The light source is positioned at the entrance of the sphere and the light emitted is reflected in all directions. This sphere is called an integrating sphere because it projects light onto the sample in all directions at constant rate. This eliminates any measurement irregularities due to shadow zones and surface faults. The wavelengths considered belong to the extended visible domain (from 360 to 740 nm). In addition, the sensitivity of the device allows breaking down the wavelength spectrum into steps of 10 nm. The light emitted by the light source can be set to different types of illuminants; we used D65 which corresponds to a temperature of 6504 K, i.e. daylight.

3.2. Measurement protocol

For wet sediment cores, the surficial layer of the sediment was removed, after which a polythene film was placed on the sample with care taken to avoid the formation of air bubbles and folds in the film. Particular attention was given to the film, since it was necessary to check that it did not alter the spectrum (Balsam et al., 1997). Contrary to the protocol proposed by Chapmann and Shackleton (1998) who recommended calibrating the spectrocolorimeter with the polythene film on the international standard white ($BaSO_4$), we used the protocol of Balsam et al. (1997) and calibrated the device without the film, since it is programmed to receive a given reflectance value for standard white. The measurement was performed with the specular component excluded (elimination of specular reflection or the "mirror effect").

3.3. L*, FDS and Q7/4 ratio

The approach proposed is based on exploiting the advantages of several calculated parameters including L*, FDS and the new Q7/4 ratio:

L* (and its equivalent optical lightness) is a fundamental parameter in colour analysis, as it describes the brightness of the sediment studied. For example, it is very often used as a routine parameter to describe sediment records during oceanographic missions (Mayer et al, 1992). However, L* does not give any information regarding the nature of the sediment.

FDS are the only tools that permit precise identification of sediment constituents (iron, carbonate, clays, etc). On the other hand, they do not permit quantifying the constituents identified.

This is why we propose a new parameter, the Q7/4 ratio (the ratio between the % reflectance value at 700nm to that at 400 nm) which provides the numerical description of the general slope of VIS. Coupled with L*, it constitutes the Q7/4 diagram used to identify the characteristic signatures of the main sediment constituents in continental, coastal and marine deposits.

4. Geological setting of the sites studied and international standard measurements

In this paper, we use the measurements performed on 8 sediment records from different environments (2 peat bogs, 3 lakes, 3 Fjords). To underline the advantage of the method, the sites studied were chosen randomly from diverse geographic, geomorphological and climatic contexts (Fig 3).

4.1. Fjords

4.1.1. Saanich Inlet, British Columbia, Canada

Saanich Inlet, British Columbia, Canada (48°35.37'N, 123°30.17'W) is a temperate fjord on the south-eastern side of Vancouver Island. It is 24 km long and its width varies from 0.4 to 7.6 km. The inlet has a maximum depth of 234 m and the mouth of the basin is partially blocked by a sill at 75 m depth. The absence of a benthic fauna as a result of anoxia leads to the preservation of annual varve-like laminae. These varves are composed of two individual laminae: the first, "silt and clay", deposited during autumn and winter, and a second, light-coloured and rich in diatoms is deposited during major spring and summer blooms. Sometimes a third, gray "clay" laminae, can be distinguished. It is interpreted as the result of flood events from the Cowichan River (Blais-Stevens et al, 2001). A 5100 cm-long piston core was retrieved and measured at 1 cm intervals with an aperture of 8 mm (Debret et al, 2006).

4.1.2. Golfe de Corcovado, Chili

In the Golfe de Corcovado, the drilling site was located at a water depth of 166 m in the centre of the basin (43°48.21'S; 073°35.02'W). A 20.69 m long Calypso core (MD07-3112) was successfully retrieved and measured at 1 cm intervals with an aperture of 8 mm.

4.1.3. Seno Reloncavi, Chili

In the Reloncavi Fjord, the drilling site was located at a water depth of 326 m in the centre of the basin (41°42.66'S; 72°46.67'W). A 21.77 m long Calypso core (MD07-3104) was successfully retrieved. It was composed of homogenous grayish olive silty clays rich in diatoms and slightly bioturbated. These sediments frequently contain shells and shell fragments. This Calypso core was measured at 1 cm intervals with an aperture of 8 mm.

4.2. Palustrine environments

4.2.1. Le Thyl, French Alps Range

Le Thyl in the French Alps Range (45°14'N, 6°29'E) is a depression located in the Maurienne valley (Savoie, France). This small peaty area (1.17 km^2) is located at the upper limit of the subalpine stage (2025 m). The inflowing catchment area (41.18 km^2) covers glacial and Quaternary sedimentary formations. The materials filling this depression are detrital at the base (150 cm thick) then become peaty up toward the surface (250 cm thick). These deposits suggest a transition from a lacustrine system to a peaty system (Mourier et al, 200). The detrital mineral materials come from occasional inflows from the catchment area whereas the peaty organic materials are produced *in situ* (acidic sphagnum peat bog). A 500 cm-long piston core was retrieved and measured at 1 cm intervals with an aperture of 8 mm.

4.2.2.   Marais de Chautagne, French Alps Range

The Marais de Chautagne (231.5 m asl.) is a marsh located between the Rhone and Lake Bourget, is regularly invaded by river water loaded with sediment during major floods. The accumulation of peat is thought to have occurred when the Rhone switched course from Lake Bourget during the Preboreal oscillation (Bravard, 1987). The lithology is composed of a peaty unit, brownish and fibrous in aspect, with many, rather large, plant remains and a fine clayey unit. A 600 cm-long piston core was retrieved and measured at 5 mm intervals with an aperture of 8 mm.

4.3. Lacustrine environments

4.3.1. Lake Bourget, French Alps Range

Lake Bourget (N45°45', E05°52'; Savoie, France) is located between the Jura and Alpine Ranges, at an altitude of 231 m asl and has a permanent catchment area of about 600 km^2.

This N-S glacial basin is 19 km long and 2.8 km wide and receives a small fraction of the discharge of the Rhone River when it leaves its partly-ice-covered alpine catchment area (Arnaud et al, 2005). The abundance of the detrital fraction has been used to reconstruct past flooding activity of the Rhone River during the Little Ice Age (Chapron et al., 2002) and over the last 7500 years (Arnaud et al., 2005). Recently, a multi-proxy study of one of the longest sedimentary records from the Alps allowed tracking detrital sources over a 10,000 year period and the reconstruction of Holocene climatic variability (Debret et al., 2010). A 1400 cm-long piston core was retrieved and measured at 5 mm intervals with an aperture of 8 mm (Debret et al., 2010).

4.3.2.   Lago Cointzio, Michoacan, Mexico

Lake Contzio (19°37'13"N; 101°15'25"W), located in central Mexico, is a small reservoir lake that covers several square kilometres during the flood period (5.5 km long, 2.2 km wide) with a maximum depth of 31.5 m (11 m on average). This lake drains formations composed of extrusive igneous rocks (basalts, andesite and ignimbrite) and andosol, acrisol, luvisol and vertisol type soils characterised by their high iron oxide/oxyhydroxide content (hematite/goethite). Core COI06-03, taken from the deepest part of the basin, was composed of alternating orange and dark layers of differing thicknesses, following a seasonal rhythm (Susperrighui et al, 2009). This 82 cm long core was extracted by a gravity corer (Uwitec Short core) and sampled every 5 mm with an aperture of 5 mm (Susperreghui, 2008).

4.3.3.   Ossa Lake, Cameroun

Ossa Lake (3°50'N ; 10°E, Cameroun) is located 35 km from the Atlantic shoreline and lies at 8 m a.s.l. It is a shallow lake, with a maximum depth of about 7 m during the wet season. With a maximum width of about 7 km, Ossa is the largest lake ($37km^2$) of the lacustrine complex on the coastal area, dominated by a swampy valley landscape. The 165 km^2 of the catchment area lies mostly on the northern side and is drained by a network of near-perennial

streams. The catchment area of Ossa Lake is a generally low-lying plain with spherical hillocks separated by steep-sided valleys. The western side of Ossa Lake is very narrow and limited by a fairly steep slope. The sedimentology of the core is a rather homogeneous deposit of dark mud with several sandy beds (Giresse et al, 2005). A core 556 cm long was extracted and measured every 5 mm, with an aperture of 8 mm for this study.

4.4. International standard measurements

To further demonstrate the efficacy of the Q7/4 diagram we used our own measurements and those that have been published, notably for iron-rich deposits (hematite and goethite signature, Balsam and Beeson, 2003; Damuth and Balsam, 2003), clay and carbonated deposits (Balsam and Beeson, 2003, Damuth and Balsam, 2003) and chlorophyll a and by products (Wolfe et al, 2006). However, in this study we have added several new reference materials, especially regarding modified organic matter for which very little data was available. For this reason we analysed samples corresponding to international standards referenced by the International Steering Committee for Black Carbon (http://mysite.du.edu/~dwismith/bcsteer.html). For the organic matter, six standard samples were measured 3 times each; a pigment (Melanoidin), two coal end-members (lignite, Beulah; bituminous coal, Pocahontas), carbonized residues (Lignocellulosic char) and grass remains (GrassChar), and two more (BL LC Char) or less oxidized (non oxidized char) mixtures of black carbon.

For clayey deposits, we used 4 international standard samples for the most common clay: montmorillonite (from Wyoming, SWy-2), chlorite ripidolite (from Romania, Chlo-Rip), chlorite containing some Talc (from Luzénac, France, Chlo-Luz), and kaolinite (from Georgia, KGa-2). These samples are natural standards referenced by the Clay Mineral Society (http://www.clays.org/SOURCE CLAYS/SCdata.html). The first two samples were compared

with industrial samples already published by Balsam and Beeson, 2003: the montmorillonite sample is API 25 from Upton, Wyoming, and is described as 100% montmorillonite (bentonite). The illite sample is API 35 (Wards 46E-4100) from Fifthian, Illinois, and is described as 100% illite. The kaolinite is compared with a sample of chalk in order to underline their different signatures and avoid confusion between them.

For iron oxide, we used 2 standard samples initially used for the clay deposit, but the high iron content allowed clearly illustrating the different oxide signatures: FOCA (Parisian Basin, montmorillonite, beidellite 70%, Kaolinite 10%, iron oxide) and Kaol-Lip (Eolians Islands, Italy) known for its clays of different colours.

5. Signatures in the Q7/4 diagram

5.1. Fjord sediments (Saanich and Corcovado fjords)

The two fjord sediment records studied have similar signatures in the form of a very elongated cloud of points characterised by variable Q7/4 ratio (from 1.5 to 6) and centred on a relatively homogeneous L* (fig. 4). This contrasted distribution made it possible to define 2 distinct poles (A and B) corresponding to extreme Q7/4 ratio values. More specifically, the reflectance of the sediments of Saanich Inlet (fig. 4) was average (in the region of 35%) with a Q7/4 ratio from 1.5 to 4. Only a few points were distinguished by reflectance values higher than 40% and of these only one point was completely separated from the general trend (L* close to 90%, Q7/4 ratio close to 1). For the fjord in Chile (fig. 5), the signature is slightly more extended with reflectance values varying from 30 to 50% and a Q7/4 ratio between 1 and 3.8.

5.2. Palustrine deposits (Chautagne and Thyl marshes)

The palustrine records have similar signatures; they form a cloud of points characterised by a Q7/4 ratio between 1 and 2.5 and by reflectance in the region of 20 to 40% (fig. 5). This

relatively homogenous distribution makes it possible to define a third pole (C) distinct from the two previous ones. The signature of the sediments of Chautagne 04 (fig. 5) corresponds to this third pole (L*: from 20 to 35%; Q7/4 ratio: from 1 to 2).

5.3. Lacustrine deposits (Lakes Bourget and Cointzio)

The lacustrine records show a more complex distribution, though common patterns can be seen (fig. 6). Thus, for each site, different sediment formations with distinct signatures can be observed. In addition, clouds of points can be seen distributed between certain of the poles (especially A and B) defined previously (figs. 4 and 5). Therefore the signatures of the sediments from Bourget (fig. 6) (L*: from 30 to 50%; Q7/4 ratio: from 15 to 4) are comparable to those defined for the fjords (fig. 4). It can also be observed that a unit of Bourget (fig. 6) has a bipolar signature, marked by a low and homogeneous Q4/7 (1.5 to 2) and highly variable reflectances (from 25 to 55%) that are comparable to those of the units of Chautagne 04 (fig. 4). However, it is noteworthy that the unit with the highest reflectance in the sediments of Lake Bourget makes it possible to define a fourth pole (D) characterised by high reflectances (< 60%) and an average Q7/4 ratio (in the region of 2).

As for Lake Cointzio, it allows the definition of a 5th pole (E) distinctly different from the previous ones, with reflectance values in the region of 40 to 50% but with very high Q7/4 reaching values around 8.

6. The Q7/4 diagram: comprehensive calibration

The comparison of different sediment records (fjords, marshes, lakes) leads to the identification of five poles (A, B, C, D and E) defined by extreme values of L* (20 to 30% and 60 to 70%) and Q7/4 (1.5 to 2 and 8 to 9). The signature of each sediment formation can therefore be described by a cloud of points close to one of the poles (the case of Lake Bourget) or drawn between two (the general case) or three poles. Thanks to recently

published works (see below), we were able to define the sedimentary significance of the 5 poles identified (fig. 7).

6.1. Pole A: "Clayey deposits"

The first pole (A) is characterised by a very low Q7/4 ratio (1.5 to 2) and intermediate L* values (from 35 to 50%). It can be identified on most of the records, particularly for Lake Bourget (fig. 6).

The signature of unit 3 of Lake Bourget is centred on pole A (fig. 6). This unit is composed of relatively coarse sediments low in carbonate (around 25%, Debret et al, 2010). They correspond to the fan of the Rhone when it flowed into Lake Bourget during the deglaciation, before filling-in the northern part of the lake and causing the river to bypass it, which is still the case today. Fluvial deposition, therefore, was responsible for the detrital clay sedimentation dominated by illite and muscovite stemming from the erosion of crystalline massifs (Debret et al., 2010).

The Saanich Inlet formations include a reference level whose signature is characteristic of this clastic pole (Fig. 4). These are clayey-silt allochthonous sediments originating in the drainage of a proglacial paleolake of the Upper Fraser Valley (Blais-Stevens et al, 2001). They are characterised by very low organic matter content and are composed of illite-muscovite clay.

The first derivative spectrum close to this pole generally shows signatures of low amplitude as indicated by the low ratio 700/400. Their spectral signatures essentially lie in wavelengths less than 400 nm characteristic of sediments rich in clay. Pole A is therefore called clayey deposits (fig. 7).

6.2. Pole B: "Chlorophyll a and by-products"

The second pole (B) is characterised by a high Q7/4 ratio (> 3) and intermediate L* values (around 40%). It is identifiable on most of the recordings, notably for the fjords and Lake

Bourget (fig. 6) which all show a vertical signature stretching from the clayey deposit poles to the second pole, i.e. pole B.

The eutrophic unit of Lake Bourget provides a characteristic signature for pole B (Fig. 5). This unit has a relatively high TOC (Total Organic Carbon) content (around 3%) and corresponds to the evolution of both the trophic and anoxic states of Lake Le Bourget during the last century (Chapron *et al.*, 1999; Giguet-Covex *et al.*, 2008).

The signature of the sediments of the Saanich Inlet is bipolar, stretching from poles A and B of the Q7/4 diagram (Fig. 5). However, the sedimentation in this basin oscillates between terrigeneous clay deposits ("clayey deposits" pole) during the rainy season and a considerable accumulation of organic matter (OM, Pole B) due to high algal production during upwelling periods (Debret et al, 2006). On the other hand, the sediments of the Saanich Inlet are contained in two assemblages: the first, closer to the clayey deposits pole, corresponds to the continuation of oxic conditions in the basin, whereas the second, closer to pole B, corresponds to the establishment of anoxic conditions at the bottom of the basin (Debret et al, 2006). In-depth examination of the first derivative spectra, characterised by a peak at 675 nm, confirms that pole B corresponds to organic-rich facies.

Pole B corresponds to a pole of organic-rich facies (Chlorophyll a and by-products) and is therefore labelled "organic rich deposits" (fig. 7).

6.3. Pole C: "Altered Organic Matter"

The third pole (C) is characterised by low L* values (< 35%) and a low Q7/4 (< 3) and is identifiable on the palustrine records (fig. 5) which all have a unit close to this pole (Q7/4 < 2). Pole C has both a low ratio and reflectance, and groups the samples corresponding to

accumulations rich in plant debris and peaty deposits, like those of the Marais de Chautagne 04 (TOC over 40%, Disnard *et al.*, 2008).

The two peat bogs have a history of rather detrital type sedimentation similar to the "clayey deposits" pole described earlier.

The peat bog at Chautagne, hemmed in by the Rhone and the lake, was formed when the Rhone filled-in the northern part of Lake Bourget during the previous glaciation, explaining the lacustrine history recorded in this core (Bravard, 1981). The peat bog at Thyl occupies a depression that had once been a lake, but was filled-in before developing the current Sphagnum peat bog (Mourier *et al.*, 2010).

As organic material is subjected to heat and/or pressure (diagenesis), its absorption band moves progressively through the VIS and into the IR, producing increasingly darker samples. This is why it is difficult to assign a pigment to this pole, as was done for Chlorophyll a. To do this it is necessary to examine the first derivative signatures in more detail (Section 7.3) Pole C in therefore labelled "altered organic matter" (fig. 7).

6.4. Pole D: "Carbonate deposits"

The fourth pole (D) is characterised by high L* values (> 50%) and an average Q7/4 (between 2 and 3). It is identifiable on the records of Lake Bourget where one unit, unit 2 (Debret et al, 2010) provides the characteristic signature. This pole had the highest L* of the sediments measured. Unit 2 of Lake Bourget corresponds to the Holocene climatic optimum where the concentration of carbonates oscillates between 40 and 60%. It is obvious that the light colour results from high carbonate content which is the main component of the sediment. The typical spectral signature is taken from a sample from Lake Bourget containing more than 50% carbonate. Pole D is therefore labelled "carbonate deposits" (fig. 7).

6.5. Pole E: "Iron-rich deposits"

The L* values of this pole are close to those of the "*Chlorophyll a and its by-products*"

but the Q7/4 values are much higher, reaching more than 8 in the case of Lake Cointzio. The

fifth pole, "E", can be seen very clearly in the record of this Mexican lake.

The lake drains a catchment area very rich in oxides (cf. part 3.3.2; Susperrighui, 2008). The

signature of the first derivate spectrum shows that the points, close to pole E, show a high

peak around 575 nm corresponding to hematite.

Pole E therefore is labelled "*Iron-rich deposits*" (fig. 7).

7. Q7/4 handbook: The importance of coupling Q7/4 and FDS analyses

This step consists in showing the importance of coupling the analysis of FDS with Q7/4,

with the goal of providing more detail to the interpretation of the poles, whether they

correspond to components of mineral (7.1) or organic (7.2) origin. The third part (7.3) deals

with the problem of composite signatures and pseudo-bipolar signatures in the Q7/4 diagram

(7.3.1), and with the superposition of the signature in the first derivative spectra (7.3.2),

notably for the organic matter spectra.

7.1. Mineral imprint

7.1.1. Iron signature

The origin of the colour in the iron oxides has been studied. The absorption bands exhibited

by the iron oxides from UV to near IR wavelengths originate from electronic transitions

within the $3d^5$ shell of the Fe^{3+} ion. These transitions are as follows: 1) Fe^{3+} ligand field

transitions, 2) transitions due to magnetically coupled Fe^{3+} cations in adjacent sites, and 3) the ligand-to-metal charge transfer (Torrent and Barron, 2002). This double excitation process usually yields the strongest band, thus it exerts a decisive influence on hue. Hence, goethite is yellow while hematite is red because the corresponding band lies at a lower wavelength in the former than in the latter (Sherman and Wait, 1985).

The detection limit for hematite and goethite when using the first derivative method is less than 0.1% in a sediment (Deaton and Balsam, 1991) or soil (Scheinost et al, 1998). This percentage is more than one order lower than the ordinary detection thresholds using x-ray diffraction. This low percentage explains that oxides are very often detected by spectrocolorimetry. In the Q7/4 diagram, the signatures will therefore be located towards the "Iron-rich deposit" pole with a very low quantity of oxide. The signature of the FDS with characteristic peaks appears at a very low concentration and quickly becomes preponderant, sometimes obscuring the signature of the embedding matrix. This situation is illustrated by the FOCA and Kaol-lip standard samples (Fig 8). Kaol-lip is a clay that not only has a high kaolinite content but also a high hematite content. This can be seen clearly in the first derivative spectrum which obscures the rest of the spectrum. In the case of the FOCA sample, a clay from the soil of the Paris basin which is a mixture of montmorillonite (70%), kaolinite (10%), iron oxide and other impurities. Here again, the signature of the clays is totally masked by the presence of goethite which prevents the signatures of the different clays from being recognized.

7.1.2. Clayey signature, Kaolinite and Carbonate

The advantage of studying the spectrocolorimetric signature of clays is to assist in the identification of the main clays by FDS analysis. We also focused on the problem raised by kaolinite, whose colour is very close to that of carbonates.

We measured 4 standard samples (kaolinite, 2 chlorites, montmorillonite) that were placed in the Q7/4 diagram (Fig 9).

Generally, the samples all have ratios lower than 2.5 but with a wide range of reflectance values (from 39 to 87%). The samples with extreme reflectance values are two chlorites. The ChPa Rip sample has the lowest reflectance due to the presence of ripidolite, a dark mineral. On the contrary, the ChLuz sample has a higher reflectance due to the presence of talc, magnesium oxide that is white. Samples SWy-2 and KGa-2 have a higher ratio in comparison to the chlorites. For the sample of Montmorillonite SWy-2, the ratio 700/400 is slightly high and is explained, according to the data sheet, by a content of Fe_2O_3 3.3%. Since detection of oxides is achieved for as little as 0.1% in content (Deaton and Balsam, 1991), this increases the 700/400 ratio towards the "Iron-rich deposits" pole.

The sample of kaolinite (KGa-2) has a ratio even higher than that of chalk (Fig 9). One reason for this rather high ratio is that the data sheet noted that the sample contained 0.98% Fe_2O_3. This content in oxide is far higher than the detection threshold, thereby explaining this ratio.

It is interesting that kaolinite, a very light coloured clay is white when pure, in comparison to a sample of chalk. Yet, their positions in the Q7/4 diagram indicate that the samples containing kaolinite and a low percentage of oxide can be confounded with the carbonate pole. This example once again illustrates the need to couple the analysis of FDS with the Q7/4 diagram since, even though both seem to have a peak at 435 nm, the peak of kaolinite is quite wide between 515 and 525 nm, whereas that of chalk is not clearly identifiable at this wavelength.

Analysis of the Q7/4 diagram and the FDS made it possible to document the signatures of the main clays, and show that FDS analysis alone permits differentiating a sample rich in kaolinite from another rich in carbonate.

7.2. Organic matter imprint

7.2.1. The signature of Chlorophyll a and by-products

High 400/700 ratios are produced by samples that exhibit significant absorption at the violet end of the spectrum, fig. 1 (Deaton *et al*, 1996). Such absorption is typically caused by immature organic material. Therefore organic-rich samples are exactly where they should be, assuming that there is immature OM characterised by the presence of chlorophyll a and its by-products (Wolfe et al., 2006). Michelluti et al, 2010 explored the concordance between measured and "inferred" chlorophyll a values, highlighted by Wolfe et al, 2006 during the study of Arctic lakes. They asked the question of whether these spectral signatures track changes of primary productivity or if they are simply records of the diagenetic signal. In their study, they critically evaluate how well VIS chlorophyll a determinations track past trends in aquatic primary production by using sediment cores from several lake systems with well-known trophic histories. Their study sites included Arctic, boreal and prairie lakes that encompassed a gradient of trophic states. In general, their spectrally inferred chlorophyll a values tracked past trends in lake trophic status consistent with historical measurements of production, or as inferred by independent proxies of primary production {Michelutti et al, 2010}. They concluded that VIS chlorophyll a proxies track the histories of lake production trends. Since primary chlorophyll a and its degradation products (pheophytin a and pheophorbide a) absorb in similar regions of the electromagnetic spectrum, the time-dependant transformation of primary sedimentary photosynthates to pheopigments does not strongly influence spectral inferences (Wolfe et al, 2006). Wolfe et al (2006) state that sedimentary concentrations of chlorophyll a below 0.05 mg/g dry mass appear sufficient to cause the development of measurable troughs in reflectance spectra.

7.2.2.   Organic compounds

The Q7/4 diagram also permits distinguishing two types of organic matter with the poles "organic rich sediment – chlorophyll a and by its products" and "altered organic deposits". The "organic rich sediment'" pole was studied in-depth as described above. However, the "altered organic matter" pole is less clearly defined. Although its Q7/4 ratio signatures appears to be homogenous, when examining the colorimetric spectra, obvious differences become apparent in the pattern of FDS. This is why we examined the FDS signatures of several international standards in order to discriminate certain signatures. Of the 6 samples measured, 3 had signatures that can be correlated with those of the peat samples studied in this paper (fig. 10).

Therefore a level measured in Thyl peat bog (acidic *Sphagnum peat bog*) has a first derivative that increases regularly in the range of 500-700 nm and correlates well with the "brown pigment", melanoidin. This pigment stems from the condensation of aldehydic sugars and amine acids produced when proteins and reducing sugars are brought in contact. This reaction mainly occurs during the humification process in soils, though in specific cases it can form in the aquatic environment (e.g. Aycard et al, 2003).

Likewise, a level of the Chautagne peat bog correlates well with the Beulah coal standard. Indeed, this "see-saw" pattern can be seen clearly in the range 600-700 nm, a region characteristic of the reflectance of organic matter. It can be assumed that this "see-saw" pattern may testify to the advanced alteration of the organic matter produced *in situ* or of erosion products of the catchment area rich in lignite.

The Chautagne peat bog also appears to share certain points with the Grass char standard. Indeed, the patterns of the range 600 - 700 nm of the two samples show numerous points of convergence. This signature seems to point to the presence of lignocellulosic matter in the bog sediments.

The samples measured in the peat bogs and in the standards therefore have common spectral characteristics that can most probably be linked to the degree of alteration of the organic matter. From a methodological viewpoint, it may be possible to improve the Q7/4 diagram for this "altered organic matter" pole, but these results above all underline the importance of coupling the signature of the first derivatives when analysing the Q7/4 diagram, in particular when in the presence of composite signatures.

7.3. Composite signatures

7.3.1. Q7/4 signature and the importance of FDS

In the Q7/4 diagram, two points located close to each other, or which are superposed, can nonetheless have different spectral signatures and thus have a totally different meanings. Let us take the example of the synthetic figure of the Q7/4 diagram and observe the signature of two very close points (Fig. 11). The first in red corresponds to Lake Cointzio in Mexico with a point measured in the detrital part of the record, while the second belongs to the eutrophised unit of Lake Bourget in France. These two samples are different although the spectocolorimetric signature of the main parameters, L* and the Q7/4 ratio, is the same. The analysis of the FDS is therefore essential for distinguishing the nature of the sediments.

The signature of the derivatives shows the very clear presence of hematite for Lake Cointzio, as indicated by the peak at 575 nm. In the range of organic matter between 600 and 700 nm, the spectral signal reproduces the "see-saw" pattern observed in the spectrum of the Beulah international standard. This therefore means that the sediment contains altered organic matter whose pigments are similar to those observed in the standard. The signal is weak in the low wavelength domain, which is quite characteristic of clayey deposits.

For Lake Bourget (curve shown in red), the signatures indicate completely different constituents since a peak at 675 nm can be seen, indicating the strong presence of pigments

linked to Chlorophyll a and its by-products, whereas the rest of the spectrum indicates the presence of carbonate whose signature weakens when the quantity of clay increases.

In terms of sediment dynamics, this means that the sedimentation of Lake Cointzio is structured around three poles, namely "altered organic deposits", "Iron-rich deposits" and "clayey deposits", whereas the sedimentation of Lake Bourget tends towards "Organic-rich sediment", "carbonated deposits" and "clayey sediment".

Therefore particular attention must be given to complex signatures and even more so when they appear to be bipolar (fig. 12). They may be structured around several poles, as emphasised by the examples of the fjords of Chile (Crocovado and Reloncavi) (fig. 12). The fjords of Reloncavi and Corcovado display apparent bipolarity between the "Iron-rich deposits" and "clayey deposits" poles. However, studying their FDS reveals more a complex composition. The signatures of the FDS indicate the presence of iron in the form of goethite, clay and OM: either altered (Pole C: with signatures that are sometimes obvious for Reloncavi, and sometimes less so for Corcovado), or less altered with the easily identifiable peak in the derivative 675nm. The bipolarity observed in the Q7/4 diagram is therefore apparent and in fact structured around 4 poles.

Thus it is vital to couple the signature of the first derivatives when analysing the Q7/4 diagram to avoid misinterpreting the diagram and improve the quality of interpretation of the sedimentary dynamics.

7.3.2. FDS imprint of a complex signature

We chose to use spectrometric data measured on the core taken from lake Ossa because it show a wide range of signatures in the organic matter domain (600-700 nm). To visualise the interaction of the different signatures with each other, we produced the schematic

representation shown in figure 13. Each corner in the square corresponds to the most representative samples of the four types of OM signature found, rather than pure poles of a particular compound: one corresponds to the "organic rich deposits – chlorophyll a and by products" pole and the three others to the "altered organic matter" pole. For the chlorophyll a and by-products pole, it was decided to choose the signature of the FDS of Lake Bourget in the eutrophised unit. The three other poles correspond to the standard samples described previously (Grass char, Beuhla and melanoidin). Of the four poles, two correspond to clearly identified pigments (chlorophyll a and melanoidin), while in the two other, the parameter involved in the colour is not clearly identified.

Lake Ossa is particularly interesting as the processes that occur in it permit both autochtone and allochton sedimentation, by the sporadic entry of the neighbouring river during flooding on the one hand, and by leaching of the catchment area on the other. The internal production of the catchment area, notably diatomic (Nguestop et al, 2004), can be seen in the signature at 675 nm of the chlorophyll a and by-products. It can, however, be found mixed with the signature identified in the Beuhla sample, for example, as demonstrated by the intermediate signal described between these two poles (left hand side of the figure). In the first intermediate signal, the signature of chlorophyll a is omnipresent and then lessens in the second with a see-saw pattern appearing after 675 nm (Fig 13). The third intermediate signal shows a very pronounced see-saw pattern where the peak at 675 nm is still present, but of the same amplitude as the other oscillations. The trough at 645 nm is the only indication of the presence in limited quantity of chlorphyll a pigments. Likewise, for the other signatures, such as melanoidin, which tend to increase from 550 nm in the FDS. The signature between 600 and 660 nm of the Grass char standard can be seen clearly in the FDS, even when it is accompanied with melanoidin (right hand side of the figure) or chlorophyll a (upper part of the figure).

Spectrocolorimetry appears to be a highly precise tool for measuring altered organic components to the point of being able to identify mixtures of different signatures. This is the first main step in view to moving towards quantitative estimation.

8. Summary, Limitations and Perspectives

The study of colour by spectrocolorimetry provides a large number of advantages, especially by permitting fast, high resolution and non destructive analysis in the field with a portable device. Several methods can be used to exploit the data resulting from spectrocolorimetry to identify the main components giving colour to sediments (factor analysis, first derivatives, etc.). However, they include disadvantages such as, notably, being mathematically cumbersome, making quantification difficult, etc. To overcome these drawbacks, this study proposes a new parameter, the Q7/4 ratio, which permits identifying both the composition of the sediment and also the sedimentary dynamics of the record when linked to L* in the same diagram and coupled with FDS analysis. The Q7/4 diagram developed offsets the disadvantages and retains the advantages of the other methods described previously. The Q7/4 diagram provides the following advantages:

-   The diagram is fast to implement and easy to set up.

-   It uses raw the data produced by the device to simplify utilisation and avoid additional calculations as much as possible. The use of the derivative, for example, removes any quantitative aspect and makes any calibration with another proxy difficult.

-   Instead of using only a chromatic (raw spectrum) or brightness (L*) parameter, Q7/4 is a combination of these two types of information given by spectrophotometry. Indeed, the samples with equivalent L* may have different compositions, so Q7/4 allows differentiating between them (e.g. Saanich Inlet). The contrary is also true

since Q7/4 does not always discriminate, and in this case L* allows differentiating sediment compositions (e.g. Chautagne).

- A diagram allows visualising the parameters represented down-core differently (in depth or in age), which is of great importance, especially when interpreting in terms of sediment dynamics.

- From a practical standpoint, the diagram must be usable on a wet sediment since one of the method's main advantages is that it is non destructive and provides high resolution. It is out of question to dry a core completely, let alone take a sample for drying. Consequently, the diagram should function with the data measured in the field (for example, on board oceanographic ships).

This study then relied on the analysis of 8 peaty, lacustrine and marginal marine sediment records with the intent of testing spectrocolorimetric measurements in the Q7/4 diagram. By coupling the diagram with the analysis of the first derivative spectra, 5 poles relating to the composition of the sediment were highlighted: (1) clayey deposits, (2) organic rich deposits (chlorophyll a and by products), (3) altered organic matter deposits, (4) iron rich deposits and, (5) carbonate deposits. We then showed the importance of coupling the Q7/4 analysis with FDS to provide greater detail in the interpretation of the poles (the example of the "altered O.M." pole), of composite signatures (the example of lakes Cointzio and Bourget) and of apparent bipolarity (Fjords of Chile), in order to underline the capacity of this tool to perform paleoclimatic/paleoenvironmental reconstructions. The Q7/4 diagram is destined to become a routine method for preliminary analysis and will permit rationalising sampling strategies.

However, much work is necessary to better understand the significance of certain FDS, such as for the "altered organic matter" pole. It is still difficult to assign a spectral signature to a level of alteration of organic matter. One of the method's disadvantages is that the presence of oxide in the sediment analysis is a problem as it can partially and even totally mask the

signature of clays. A possible progression of the method would be to incorporate spectral deconvolution to remove the signature of the oxides and reveal other constituents. If possible such deconvolution would constitute the first step towards quantification. The latter is applicable to only a few specific cases and thus represents an additional hurdle to overcome.

Acknowledgements :

References

Arimoto, R., Balsam, W., & Schloesslin, C. (2002). Visible spectroscopy of aerosol particles collected on filters: Iron-Oxide minerals. *Atmospheric Environment*, *36*(1), 89-96.

Arnaud, F., Revel, M., Chapron, E., Desmet, M., & Tribovillard, N. (2005). 7200 years of rhone river flooding activity in lake le bourget, france: A high-resolution sediment record of NW alps hydrology. *Holocene*, *15*(3), 420-428. doi:10.1191/0959683605hl801rp

Aycard, M., Derenne, S., Largeau, C., Mongenot, T., Tribovillard, N., & Baudin, F. (2003). Formation pathways of proto-kerogens in holocene sediments of the upwelling influenced cariaco trench, venezuela. *Organic Geochemistry*, *34*(6), 701-718.

Bahr, A., Lamy, F., Arz, H., Kuhlmann, H., & Wefer, G. (2005). Late glacial to holocene climate and sedimentation history in the NW black sea. *Marine Geology*, *214*(4), 309-322. doi:10.1016/j.margeo.2004.11.013

Balsam, W., Ji, J., & Chen, J. (2004). Climatic interpretation of the luochuan and lingtai loess sections, china, based on changing iron oxide mineralogy and magnetic susceptibility. *Earth and Planetary Science Letters*, *223*(3-4), 335-348. doi:10.1016/j.epsl.2004.04.023

Balsam, W. L., & Beeson, J. P. (2003). Sea-Floor sediment distribution in the gulf of mexico. *Deep Sea Research Part I: Oceanographic Research Papers*, *50*(12), 1421-1444. doi:10.1016/j.dsr.2003.06.001

Balsam, W.L. and B.C. Deaton, 1991. Sediment dispersal in the Atlantic Ocean: Evaluation by visible light spectra. Reviews in Aquatic Sciences, 4:411-447.

Balsam, W. L., & Deaton, B. C. (1996). Determining the composition of late quaternary marine sediments from NUV, VIS, and NIR diffuse reflectance spectra. *Marine Geology*, *134*(1-2), 31-55.

Balsam, W.L., Damuth, J.E., Schneider, R.R., 1997. Comparison of shipboard vs shore-based spectral data from Amazon Fan cores: implications for interpreting sediment composition. Ocean Drill. Program Sci. 155s, 193–215.

Balsam, W. L., Deaton, B. C., & Damuth, J. E. (1998). The effects of water content on diffuse reflectance spectrophotometry studies of deep-sea sediment cores. *Marine Geology*, *149*(1-4), 177-189.

Balsam, W. L., Deaton, B. C., & Damuth, J. E. (1999). Evaluating optical lightness as a proxy for carbonate content in marine sediment cores. *Marine Geology*, *161*(2-4), 141-153.

Balsam, W. L., and Deaton, B. C. (1991). Sediment dispersal in the Atlantic-ocean − Evaluation by visible-light spectra. *Reviews in Aquatic Sciences*, *4*(4), 411-447.

Balsam, W.L., Deaton, B.C., Full, W.E., Hurley, P., 1986. Evidence of transport and redistribution of Atlantic surficial sediment from visible light spectra. *Geol. Soc. Am. Abstr. Programs* 18: 533.

Barranco, F. T., Balsam, W. L., & Deaton, B. C. (1989). Quantitative reassessement of brick red lutites − Evidence from réflectance spectrophotometry. *Marine Geology*, *89*(3-4),

299-314.

Barrett, L. R. (2002). Spectrophotometric color measurement in situ in well drained sandy soils. *Geoderma*, *108*(1-2), 49-77.

Blais-Stevens, A., Bornhold, B. D., Kemp, A. E. S., Dean, J. M., & Vaan, A. A. (2001). Overview of late quaternary stratigraphy in saanich inlet, british columbia: Results of ocean drilling program leg 169S. *Marine Geology*, *174*(1-4), 3-26.

Boes, X., Piotrowska, N., & Fagel, N. (2005). High-Resolution diatom/clay record in lake baikal from grey scale, and magnetic susceptibility over holocene and termination I. *Global and Planetary Change*, *46*(1-4), 299-313. doi:10.1016/j.gloplacha.2004.09.025

Bozzano, G., Kuhlmann, H., & Alonso, B. (2002). Storminess control over african dust input to the moroccan atlantic margin (NW africa) at the time of maxima boreal summer insolation: A record of the last 220 kyr. *Palaeogeography, Palaeoclimatology, Palaeoecology*, *183*(1-2), 155-168.

Bravard, J.P., 1981. La Chautagne, dynamique de l'environnement d'un pays savoyard. Thèse de doctorat. Institut des Etudes Rhodaniennes des Universités de Lyon. Mem. & Doc 18, p182.

Bravard, J.-P., 1987. Le Rhône, Du Léman à Lyon. Editions La Manufacture, Lyon.

Chapman, M. R., & Shackleton, N. J. (1998). What level of resolution is attainable in a deep-sea core : Results of a Spectrophotometer Study. *Paleoceanography*, *13*, 311-315.

Chapron, E., Fain, X., Magand, O., Charlet, L., Debret, M., & Melieres, M. A. (2007). Reconstructing recent environmental changes from proglacial lake sediments in the western alps (lake blanc huez, 2543 m a.s.l., Grandes rousses massif, france). *Palaeogeography, Palaeoclimatology, Palaeoecology*, *252*(3-4), 586-600. doi:10.1016/j.palaeo.2007.05.015

Chapron, E., Beck, C., Pourchet, M., & Deconinck, J. F. (1999). 1822 earthquake-triggered homogenite in lake le bourget (NW alps). *Terra Nova*, *11*(2-3), 86-92.

Chapron, E., Desmet, M., De Putter, T., Loutre, M. F., Beck, C., & Deconinck, J. F. (2002). Climatic variability in the northwestern alps, france, as evidenced by 600 years of terrigenous sedimentation in lake le bourget. *Holocene*, *12* (2), 177-185. doi:10.1191/0959683602h1520rp

Cohen, M. C. L., Guimarães, J. T. F., França, M., Lara, R. J., & Behling, H. (2009). Tannin as an indicator of paleomangrove in sediment cores from amapá, northern brazil. *Wetlands Ecology and Management*, *17*(2), 145-155. doi:10.1007/s11273-008-9100-z

Damuth, J. E., & Balsam, W. L. (2003). 7. Data report: Spectral data from sites 1165 and 1167 including the hirisc section from hole 1165B. *Proceedings of the Ocean Drilling Program, Scientific Results*, *188*.

Das, B., Vinebrooke, R. D., Sanchez-Azofeifa, A., Rivard, B., & Wolfe, A. P. (2005).

Inferring sedimentary chlorophyll concentrations with reflectance spectroscopy: A novel approach to reconstructing historical changes in the trophic status of mountain lakes. *Canadian Journal of Fisheries and Aquatic Sciences*, *62*(5), 1067-1078. doi:10.1139/F05-016

Deaton, B.C., 1987. Quantification of rock color from Munsell chips. J. Sediment. Res. 57 (4): 774-776.

Deaton, B. C., and Balsam, W. L. (1991). Visible spectroscopy – a rapid method for determining hématite and goethite concentration in geological materials. *Journalof sedimentary geology*, *61*(4), 628-632.

Deaton, B. C., & Balsam, W. L. (1996). Determination of metalloporphyrins in rocks, sediments and other geological materials using total reflectance spectrophotometry. *Organic Geochemistry*, *24*(3), 323-331.

Deaton, B. C., Nestell, M., & Balsam, W. L. (1996). Spectral reflectance of conodonts: A step toward quantitative color alteration and thermal maturity indexes. *AAPG Bulletin-American Association of Petroleum Geologists*, *80*(7), 999-1007.

Debret, M., Chapron, E., Desmet, M., Rolland-Revel, M., Magand, O., Trentesaux, A., Bout-Roumazeille, V., Nomade, J., Arnaud, F. (2010). North western alps holocene paleohydrology recorded by flooding activity in lake le bourget, france. *Quaternary Science Reviews*, *29*(17-18), 2185-2200. doi:10.1016/j.quascirev.2010.05.016

Debret, M., Desmet, M., Balsam, W., Copard, Y., Francus, P., & Laj, C. (2006). Spectrophotometer analysis of holocene sediments from an anoxic fjord: Saanich inlet, british columbia, canada. *Marine Geology*, *229*(1-2), 15-28. doi:10.1016/j.margeo.2006.01.005.

Disnar, J. R., Jacob, J., Morched-Issa, M., Lottier, N., & Arnaud, F. (2008). Assessment of peat quality by molecular and bulk geochemical analysis: Application to the holocene record of the chautagne marsh (haute savoie, france). *Chemical Geology*, *254*(1-2), 101-112. doi:10.1016/j.chemgeo.2008.06.004

Dubois, N., Kindler, P., Spezzaferri, S., & Coric, S. (2008). The initiation of the southern central great barrier reef: New multiproxy data from pleistocene distal sediments from the marion plateau (NE australia). *Marine Geology*, *250*(3-4), 223-233. doi:10.1016/j.margeo.2008.01.007

Ellwood, E., & Brooks, B. (1995). Magnetic and geochemical variations as indicators of palaeoclimate and archaeological site evolution: Examples from 41TR68, fort worth, texas. *Journal of Archaeological Science*, *22*(3), 409-415.

Ellwood, B.B., Peter, D.E., Balsam, W., and Schieber, J., 1995. Magnetic and geochemical variations as indicators of paleoclimatic and archaeological site evolution: Examples from 41TR68, Fort Worth, Texas. Journal of Archaeological Science, 22:409-415.

Giguet-Covex, C., Arnaud, F., Poulenard, J., Enters, D., Reyss, J. L., Millet, L., . . . Vidal, O.

(2010). Sedimentological and geochemical records of past trophic state and hypolimnetic anoxia in large, hard-water lake bourget, french alps. *Journal of Paleolimnology*, *43*(1), 171-190. doi:10.1007/s10933-009-9324-9

Giosan, L., Flood, R. D., & Aller, R. C. (2002). Paleoceanographic significance of sediment color on western north atlantic drifts: I. Origin of color. *Marine Geology*, *189*(1-2), 25-41.

Giosan, L., Flood, R. D., Grützner, J., Franz, S. O., Poli, M. S., & Hagen, S. (2001). 6. High-Resolution carbonate content estimated from diffuse spectral reflectance for leg 172 sites. In Keigwin, L.D., Rio, D., Acton, G.D., and Arnold, E. (Eds.) *Proceedings of the Ocean Drilling Program, Scientific Results* Volume 172, pp 1-12.

Giresse, P., Maley, J., & Kossoni, A. (2005). Sedimentary environmental changes and millennial climatic variability in a tropical shallow lake (lake ossa, cameroon) during the holocene. *Palaeogeography, Palaeoclimatology, Palaeoecology*, *218*(3-4), 257-285.

Guedes, A., Ribeiro, H., Valentim, B., and Noronha, F. (2009). Quantitative colour analysis of beach and dune sediments for forensic applications: A portuguese example. *Forensic Science International*, *190*(1-3), 42-51. doi:10.1016/j.forsciint.2009.05.010

Helmke, J. P., Schulz, M., & Bauch, H. A. (2002). Sediment-Color record from the northeast atlantic reveals patterns of millennial-scale climate variability during the past 500,000 years. *Quaternary Research*, *57*(1), 49-57. doi:10.1006/qres.2001.2289

Hepp, D. A., Mörz, T., & Grützner, J. (2006). Pliocene glacial cyclicity in a deep-sea sediment drift (antarctic peninsula pacific margin). *Palaeogeography, Palaeoclimatology, Palaeoecology*, *231*(1-2), 181-198. doi:10.1016/j.palaeo.2005.07.030

Horneman, A., Van Geen, A., Kent, D. V., Mathe, P. E., Zheng, Y., Dhar, R. K., O'Connell, S., Hoque, M. A., Aziz, Z., Shamsudduha, M., Seddique, A.A., and Ahmed, K. M. (2004). Decoupling of as and fe release to bangladesh groundwater under reducing conditions. Part I: Evidence from sediment profiles1. *Geochimica Et Cosmochimica Acta*, *68*(17), 3459-3473. doi:10.1016/j.gca.2004.01.026

Ji, J, Shen, J., Balsam, W., and Chen, J, Liu, L., Liu, X. 2005. Asian Monsoon oscillations in the northeastern Qinghai-Tibet Plateau since the late glacial as interpreted from visible reflectance of Qinghai Lake sediments. Earth and Planetary Science Letters. 233:61-70

Jin, Z. D., Wu, Y., Zhang, X., & Wang, S. (2005). Role of late glacial to mid-holocene climate in catchment weathering in the central tibetan plateau. *Quaternary Research*, *63*(2), 161-170. doi:10.1016/j.yqres.2004.09.012

Khan, M. A., Ueno, K., Horimoto, S., Komai, F., Someya, T., Inoue, K., Tanaka, K. and Ono, Y. (2009). CIELAB color variables as indicators of compost stability. *Waste Management (New York, N.Y.)*, *29*(12), 2969-75. doi:10.1016/j.wasman.2009.06.021

Kirby, C. S., Decker, S. M., & Macander, N. K. (1999). Comparison of color, chemical and mineralogical compositions of mine drainage sediments to pigment. *Environmental*

Geology, *37*(3), 243-254.

Koptíková, L., Bábek, O., Hladil, J., Kalvoda, J., & Slavík, L. (2010). Stratigraphic significance and resolution of spectral reflectance logs in lower devonian carbonates of the barrandian area, czech republic; a correlation with magnetic susceptibility and gamma-ray logs. *Sedimentary Geology*, *225*(3-4), 83-98. doi:10.1016/j.sedgeo.2010.01.004

Kovalev, A. A., & Nichiporovich, N. Z. A. (2003). Spectrophotometric characteristic of peat having various origins and degrees of decomposition. *Journal of Applied Spectroscopy*, *70*, 365-371. doi:UDC 552.577:535.312(476)

Lovelock, C. E., & Robinson, S. A. (2002). Surface reflectance properties of antarctic moss and their relationship to plant species, pigment composition and photosynthetic function. *Plant, Cell & Environment*, *25*(10), 1239-1250.

Martínez-Carreras, N., Udelhoven, T., Krein, A., Gallart, F., Iffly, J. F., Ziebel, J., Hoffmann, L., Pfister, L., Walling, D. E. (2010). The use of sediment colour measured by diffuse reflectance spectrometry to determine sediment sources: Application to the attert river catchment (luxembourg). *Journal of Hydrology*, *382*(1-4), 49-63. doi:10.1016/j.jhydrol.2009.12.017

Michelutti, N., Blais, J. M., Cumming, B. F., Paterson, A. M., Rühland, K., Wolfe, A. P., & Smol, J. P. (2010). Do spectrally inferred determinations of chlorophyll a reflect trends in lake trophic status? *Journal of Paleolimnology*, *43*(2), 205-217. doi:10.1007/s10933-009-9325-8

Miralles, I., Ortega, R., Sánchez-Mara\cn\ckn, M., Soriano, M., & Almendros, G. (2007). Assessment of biogeochemical trends in soil organic matter sequestration in mediterranean calcimorphic mountain soils (almería, southern spain). *Soil Biology and Biochemistry*, *39*(10), 2459-2470. doi:10.1016/j.soilbio.2007.04.017

Mix, A. C., Harris, S. E., & Janecek, T. R. (1995). Estimating lithology from nonintrusive reflectance spectra: Leg 138. In *Proceedings of the ocean drilling program, scientific results.*

Mix, A. C., Rugh, W., Pisias, N. G., & Veirs, S. (1992). Color reflectance spectroscopy: A tool for rapid characterization of deep-sea sediments. *Proceedings of the Ocean Drilling Program, Initial Reports*, *138*, 67-77.

Mourier, B., Poulenard, J., Carcaillet, C., & Williamson, D. (2010). Soil evolution and subalpine ecosystem changes in the french alps inferred from geochemical analysis of lacustrine sediments. *Journal of Paleolimnology*, *44*(2), 571-587. doi:10.1007/s10933-010-9438-0

Murphy, R.J., Underwood, A.J., Pinkerton, M.H., Range, P., 2005. Field spectrometry: New methods to investigate epilithic micro-algae on rocky shores. *J. Exp. Mar. Biol. Ecol.* 325 (1): 111-124.

Nguetsop, V. F., Servant-Vildary, S., & Servant, M. (2004). Late holocene climatic changes

in west africa, a high resolution diatom record from equatorial cameroon. *Quaternary Science Reviews*, *23*(5-6), 591-609.

Ortiz, J. D., O'Connell, S., & Mix, A. C. (1999). Data report: Spectral reflectance observations from recovered sediments. In *Proceedings of the ocean drilling program, scientific results.*

Ortiz, J. D., Polyak, L., Grebmeier, J. M., Darby, D., Eberl, D. D., Naidu, S., & Nof, D. (2009). Provenance of holocene sediment on the chukchi-alaskan margin based on combined diffuse spectral reflectance and quantitative x-ray diffraction analysis. *Global and Planetary Change*, *68*(1-2), 73-84. doi:10.1016/j.gloplacha.2009.03.020

Piper, D. J. W., & Hundert, T. (2002). Provenance of distal sohm abyssal plain sediments: History of supply from the wisconsinan glaciation in eastern canada. *Geo-Marine Letters*, *22*(2), 75-85. doi:10.1007/s00367-002-0101-2

Rein, B., Sirocko, F., (2002). In-situ reflectance spectroscopy: analysing techniques for high-resolution pigment logging in sediment cores. *Int. J. Earth Sci.* 91: 950-954.

Roth, S., & Reijmer, J. J. G. (2005). Holocene millennial to centennial carbonate cyclicity recorded in slope sediments of the great bahama bank and its climatic implications. *Sedimentology*, *52*(1), 161-181. doi:10.1111/j.1365-3091.2004.00684.x

Rothwell, R.G., Rack, F.R., (2006). New techniques in sediment core analysis: an introduction. Geological Society, London, *Special Publications* 267: 1-29.

Sánchez-Marañón, M., Delgado, G., Melgosa, M., Hita, E., Delgado, R., (1997). CIELab color parameters and their relationship to soil characteristics in Mediterranean red soils. *Soil Sci.* 162 (11): 833-842.

Sánchez-Marañón, M., Soriano, M., Melgosa, M., Delgado, G., Delgado, R., (2003). Quantifying the effects of aggregation, particle size and components on the colour of Mediterranean soils. *Eur. J. Soil Sci.* 55: 551-565.

Sánchez-Marañón, M., Ortega, R., Miralles, I., Soriano, M., (2007). Estimating the mass wetness of Spanish arid soils from lightness measurements. *Geoderma* 141: 397–406

Scheinost, A. C., Chavernas, A., Barron, V., & Torrent, J. (1998). Use and limitations of second-derivative diffuse reflectance spectroscopy in the visible to near-infrared range to identify and quantity fe oxide minerals in soils. *Clays and Clay Minerals*, *46*(5), 528-536.

Shen, Z. X., Cao, J. J., Zhang, X. Y., Arimoto, R., Ji, J. F., Balsam, W. L., Wang, Y. Q., Zhang, R. J. and Li, X. X. (2006). Spectroscopic analysis of iron-oxide minerals in aerosol particles from northern china. *The Science of the Total Environment*, *367*(2-3), 899-907. doi:10.1016/j.scitotenv.2006.01.003

Sherman, D. M., & Waite, T. D. (1985). Electronic-Spectra of fe-3+ oxides and oxide hydroxides in the near ir to near uv. *American Mineralogist*, *70*(11-12), 1262-1269.

Shields, J. A., Arnaud, R., Paul, E. A., & Clayton, J. S. (1966). Measurement of soil color. *Can. J. Soil Sci*, *46*, 83-90.

Schneider, R.R., Cramp, A., Damuth, J.E., Hiscott, R.N., Kowsmann, R.O., Lopez, M., Nanayama, F., Normark, W.R., Shipboard Scientific Party (1995). Color-reflectance measurements obtained from leg 155 cores. In: Flood, R.D., Piper, D.J.W., Klaus, A., et al. (Eds.), Proc. ODP, Init. Repts., vol. 155. Ocean Drilling Program, College Station, TX, pp. 1–65.

Susperregui, A.S., Gratiot, N., Esteves, M. and Prat, C. (2009). A preliminary hydrosedimentary view of a highly turbid, tropical, manmade lake: Cointzio Reservoir (Michoacán, Mexico). Lakes & Reservoirs : Res & Management (14), 31-39.

Susperregui, A.S. (2008). Caractérisation hydro-sédimentaire des retenues de Cointzio et d'Umécuaro (Michoacán, Mexique) comme indicateur du fonctionnement érosif du bassin versant. Phd These from Joseph Fourier University, 289 pp.

Tiljander, M., Ojala, A., Saarinen, T., & Snowball, I. (2002). Documentation of the physical properties of annually laminated (varved) sediments at a sub-annual to decadal resolution for environmental interpretation. *Quaternary International*, *88*, 5-12.

Torrent, J., & Barrón, V. (2002). Diffuse reflectance spectroscopy of iron oxides. *Encyclopedia of Surface and Colloid Science*, 1438-1446.

Wang, D., Dowell, F. E., & Lacey, R. E. (1999). Single wheat kernel color classification by using near-infrared reflectance spectra. *Cereal Chemistry*, *76*(1), 30-33.

Von Gunten, L., Grosjean, M., Rein, B., Urrutia, R., Appleby, P., 2009. A quantitative high-resolution summer temperature reconstruction based on sedimentary pigments from Laguna Aculeo, central Chile, back to AD 850. *Holocene* 19 (6): 873-881.

Weber, M. E., Tougiannidis, N., Kleineder, M., Bertram, N., Ricken, W., Rolf, C., Reinsch, T., and Antoniadis, P. (2010). Lacustrine sediments document millennial-scale climate variability in northern greece prior to the onset of the northern hemisphere glaciation. *Palaeogeography, Palaeoclimatology, Palaeoecology*. doi:10.1016/j.palaeo.2010.03.007

Weber, M. E. (1998). Estimation of biogenic carbonate and opal by continuous non-destructive measurments in deep-sea sediments: Application to the eastern equatorial Pacific. *Deep-Sea Research Part 1*, *45*, 1955-1975.

Wilson, L.J., Austin, W.E.N., 2002. Millennial and sub-millennial-scale variability in sediment colour from the Barra Fan, NW Scotland: implications for British ice sheet dynamics. Geological Society, London, *Special Publications* 203: 349-365.

Wolf-Welling, T. C. W., Cowan, E. A., Daniels, J., Eyles, N., Maldonado, A., & Pudsey, C. J. (2001). Data report: Diffuse spectral reflectance data from rise sites 1095, 1096, and 1101 and Palmer Deep sites 1098 and 1099 (leg 178, western antarctic peninsula.). *Proc. ODP, sci. Results*.

Wolfe, A. P., Vinebrooke, R. D., Michelutti, N., Rivard, B., & Das, B. (2006). Experimental calibration of lake-sediment spectral reflectance to chlorophyll a concentrations: Methodology and paleolimnological validation. *Journal of Paleolimnology*, *36*(1), 91-100. doi:10.1007/s10933-006-0006-6

Yu, Y., Yang, T., Li, J., Liu, J., An, C., Liu, X., Fan, Z., Lu, Z., Li, Y., and Su, X. (2006). Millennial-Scale holocene climate variability in the NW china drylands and links to the tropical pacific and the north atlantic. *Palaeogeography, Palaeoclimatology, Palaeoecology*, *233*(1-2), 149-162. doi:10.1016/j.palaeo.2005.09.008

Zhang, Y. G., Ji, J., Balsam, W. L., Liu, L., & Chen, J. (2007). High resolution hematite and goethite records from ODP 1143, south china sea: Co-Evolution of monsoonal precipitation and El Niño over the past 600,000 years. *Earth and Planetary Science Letters*, *264*(1-2), 136-150. doi:10.1016/j.epsl.2007.09.022

Zhou, W., Chen, L., Zhou, M., Balsam, W. L., & Ji, J. (2010). Thermal identification of goethite in soils and sediments by diffuse reflectance spectroscopy. *Geoderma*, *155*(3-4), 419-425. doi:10.1016/j.geoderma.2010.01.00
Figure Caption :

Figure Captions

Figure 1 : CIELab spherical referential. L* (white/black), a* (red/green) and b* (yellow/blue) are the three axis.

Figure 2. Upper part, data in blue correspond to raw data coming from spectrophotometer in this visible wavelength (400 to 700 nm). The first derivatives values (red curve) allowed to identify majority components contributing to sediment color (600 à 700 nm range corresponds to organic matter domain). Down-core first derivative spectrum (lower part) permit, in Lake Le Bourget for example, to distinguish various facies. 675 first derivative values present in eutrophic unit, represents the first organic facies, facies 2 and 3 correspond to carbonate unit and the last unit is dominated with clayey signatures.

Figure 3 : Location of the various sites used for Q7/4 diagram calibration and validation. 3 lakes, 2 peats et 3 fjords were studied for their sedimentological content and measured by spectrophotometry.

Figure 4 : Q7/4 diagram for palustrine environments with on the left, Thyl peat (Alps range, France) and on the right Chautagne peat (Alpine valley, France).

Figure 5 : Q7/4 Diagram for fjords environments, with on the left, Saanich Inlet (British Columbia, Canada) and on the right Corcovado fjord (Chile).

Figure 6 : Q7/4 Diagram for lacustrine environments, with on left Lake Le Bourget (Alpine Valley, France) and on the right Coïntzio Lake, Mexico.

Figure 7. Q7/4 diagram for wet sediment combined with FDS allowed to distinguish 5 poles : Clayey deposits, organic rich deposits (Chlorophyll a and by products), Altered organic matter deposits, Iron rich deposits, carbonated deposits. FDS analysis give more details in the signature of some pole like for Iron-rich deposits and Altered organic matter pole.

Figure 8 : 3 international standards are compared with various samples from Chautagne and Thyl peat highlight various pattern that allowed distinguishing different types of organic matter. For the last 3 others standards, they were not observed in the various records however their analyses reinforced the usefulness of the tools because it is possible to differentiate coal, charcoal, soot, black carbon in spite of a very low reflectance.

Figure 9 : Two points, however, side by side, may carry different information. Effectively Cointzio Lake in red and Lake Le Bourget in Blue suggest points close to each other. However, looking at the FDS (top right), the composition of the samples is clearly different with a 675 nm peak and a typical trend for carbonates Bourget cons a major peak in hématite and altered organic matter signal for Cointzio Lake. This example highlights the need to couple FDS and Q7/4 diagram to approach the analysis of sediment dynamics.

Figure 10 : Illustration of the special care on the cloud point distributions when an apparent bipolarity is observe. FDS Analysis reveals a much more complex system that implies 4 poles. On the left, the Reloncavi fjord indicates an organization around 4 poles as confirmed by FDS analysis (top and bottom). In the Corcovado Gulf, values seem rather organized around three major poles, the Iron rich deposition pole being less present.

Figure 11 : Hematite FDS highlight a major peak around 575 nm whereas goethite can be recognized with the two peaks around 435 nm and 545 nm.

Figure 12 : Position of chalk and clay standard samples in Q7/4 diagram. FDS of these samples allowed to clearly identify the different clays and to distinguish kaolinite and carbonates signature that are very close in Q7/4 diagram.

Figure 13 : Block diagram illustrating the superposition of different FDS from fresh and altered organic matter in sediments from Lake Ossa. The 4 corners of the square correspond to differing states of organic matter as expressed in FDS: the pigments of chlorophyll a and melanoidin, the ligniocellulosic compounds (Grass char) and lignite (Beuhla).

Table 1. Synthesis of the different methods used in spectrophotorimetry. Are summarized in the table: the benefits, pitfalls, applications accompanied by an example and reference concerned. The three methods described in this article are in bold.
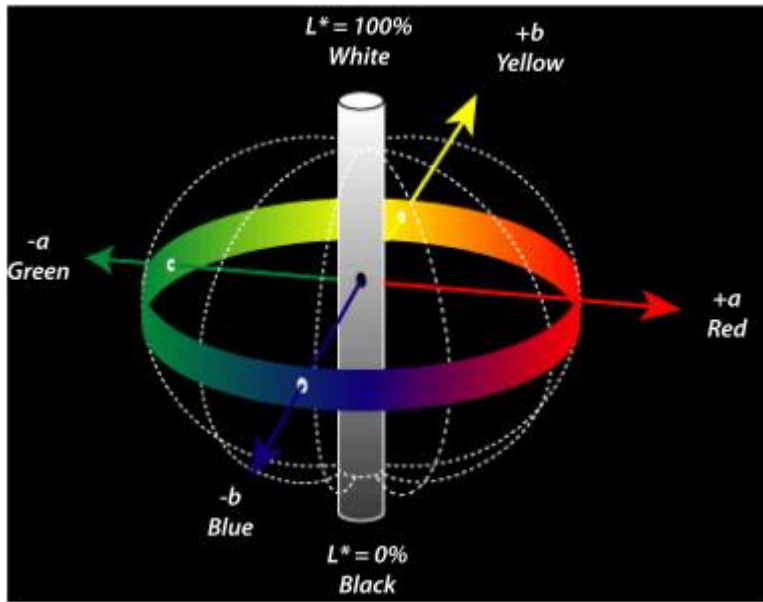
Fig. 1. : CIELab spherical referential. L* (white/black), a* (red/green) and b* (yellow/blue) are the three axis.
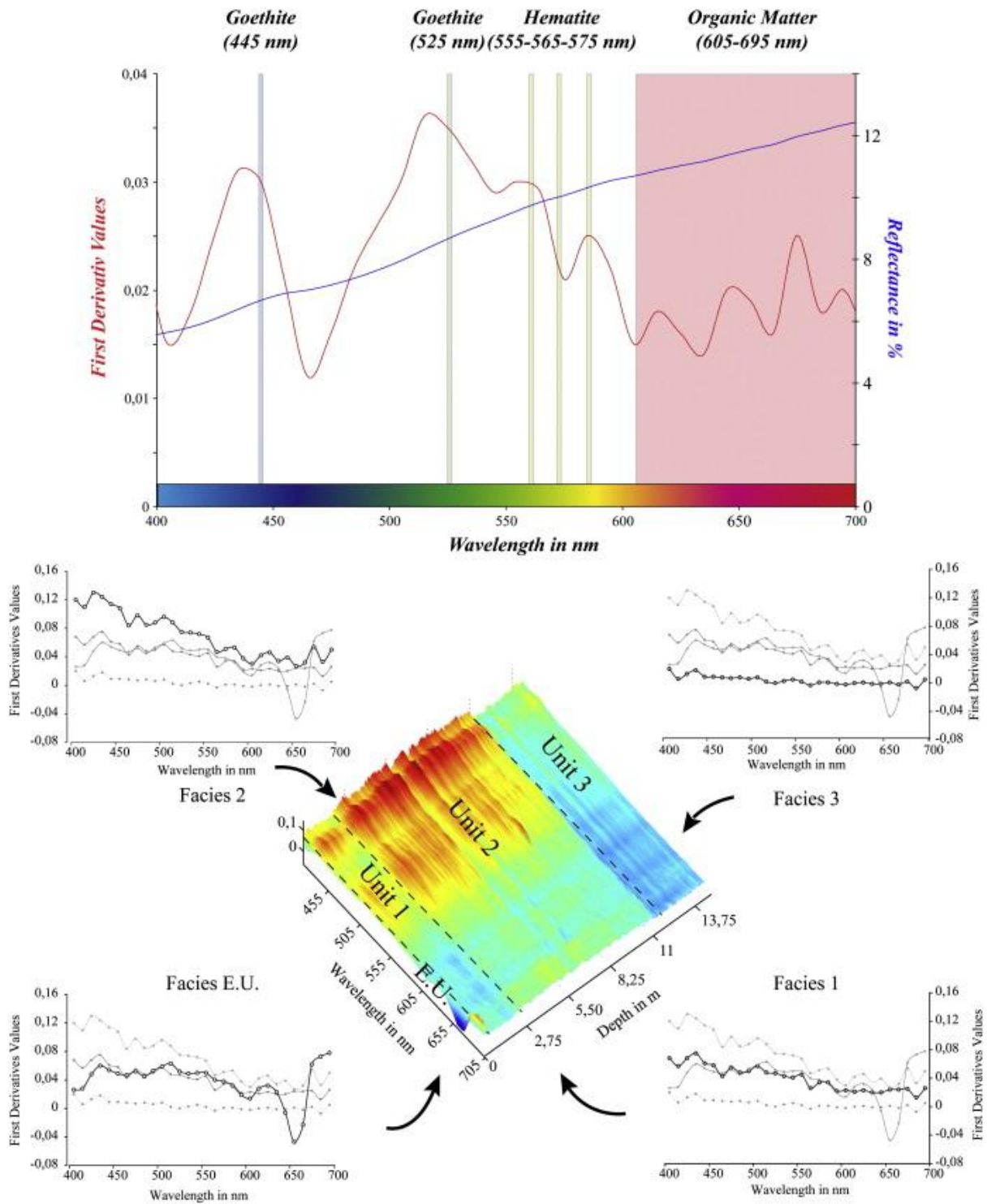
Fig. 2. : Upper part, data in blue correspond to raw data coming from spectrophotometer in this visible wavelength (400 to 700 nm). The first derivative values (red curve) allowed to identify majority components contributing to sediment color (600–700 nm range corresponds to organic matter domain). Down-core first derivative spectrum (lower part) permits, in Lake Le Bourget for example, to distinguish various facies. 675 first derivative values present in eutrophic unit, represent the first organic facies, facies 2 and 3 correspond to carbonate unit and the last unit is dominated with clayey signatures.

Table 1. Synthesis of the different methods used in spectrophotorimetry. The benefits, pitfalls, applications accompanied by an example and reference concerned are summarised in the table. The three methods described in this article are in bold.

| Methods	Advantages	Disadvantages	Applications	Example	References
CIELab referential	Calibration with geochemical measurements	Calibration limited to mixtures of two constituents	Facies characterisation	a*: iron oxide content	Helmke et al., 2002
			Qualitative identification	b*: diatoms vs terrigenous	Debret et al., 2006
			Quantification if calibrated with geochemistry	L*: Aragonite amount	Roth and Reijmer, 2005
Raw Spectrum	Raw data, no mathematical processing	No identification of constituents	Facies characterisation	Effect of water content on sediment	Balsam et al., 1997
Frequencies gathering	Fast and easy to process	Limited to mixtures of colour-contrasted constituents	Facies characterisation	Redness rating: oxide	Ji et al., 2005
			Relative quantification	Hematite Goethite ratio	Zhang et al., 2007
First Derivatives methods	Identification of the dominant coloured constituents (example: 675 nm: Chlorophyll a)	No quantitative information	Facies characterisation	Sediment cartography	Balsam and Beeson, 2003
		Similar spectra for various mixture of the same constituents		Reconstruction of paleoproductivity.	Wolfe et al., 2006
		Useful for dry sediment			
Factor analyses	Combination with other sedimentological large data set	Complex statistical method	Facies characterisation	Clays and oxide identification in various environment	Ortiz et al., 2009
		Constituents found together will appear in the same factor	Qualitative identification		Damuth and Balsam, 2003
			Quantification if calibrated with geochemistry		
Q7/4 Diagram	Fast and easy to process (Raw data)	2D representation (Not vs time or in-depth)	Facies characterisation	Analyses of sedimentary dynamics in various continental and marine environments (Lakes, Fjords, Peatlands, Marsh, Oceanic sediments)	This study
	Combination of brightness (L*) and chromatic information (Raw spectrum)	Only calibrated for wet sediment (actually)	Qualitative identification		
	Useful for wet sediment		Relative quantification		
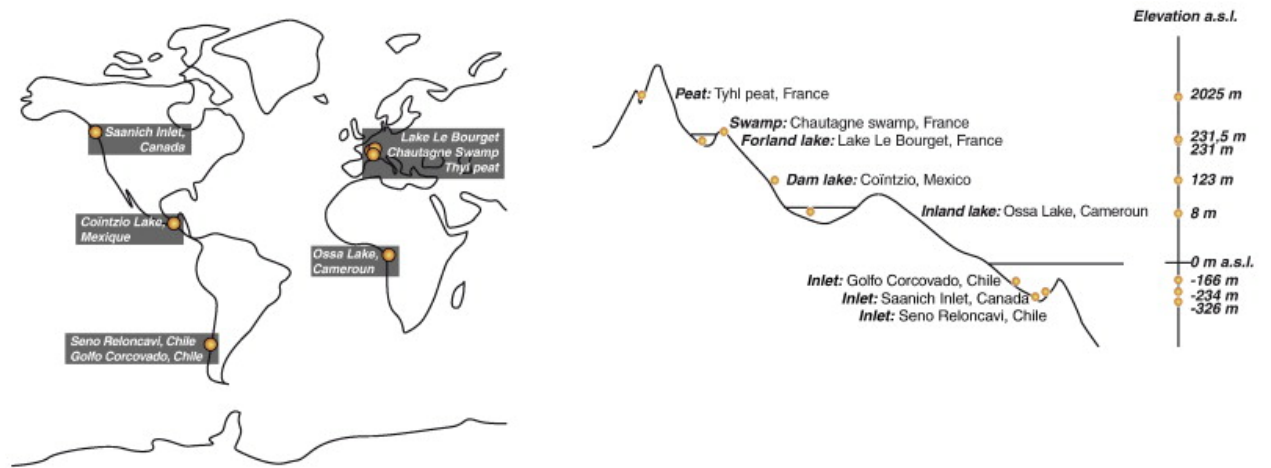
Fig. 3. : Location of the various sites used for Q7/4 diagram calibration and validation. 3 lakes, 2 peats and 3 fjords were studied for their sedimentological content and measured by spectrophotometry.
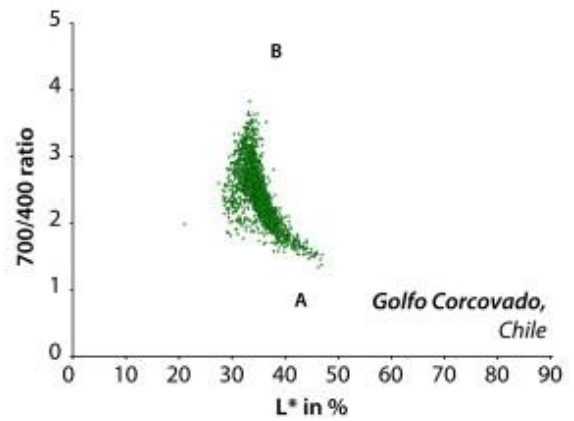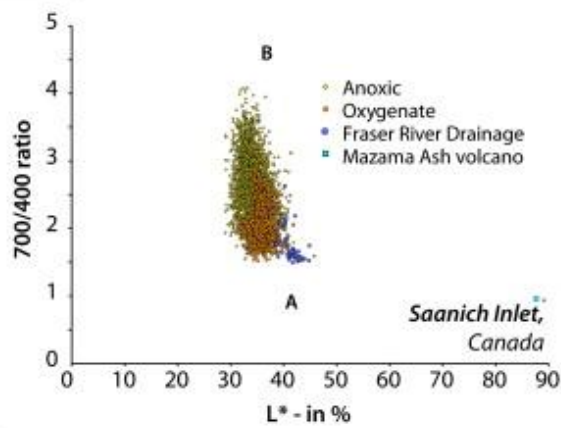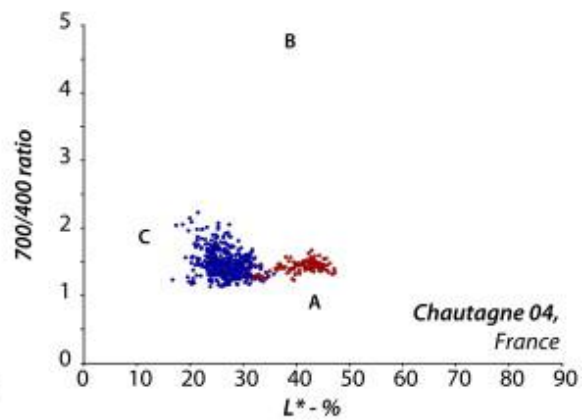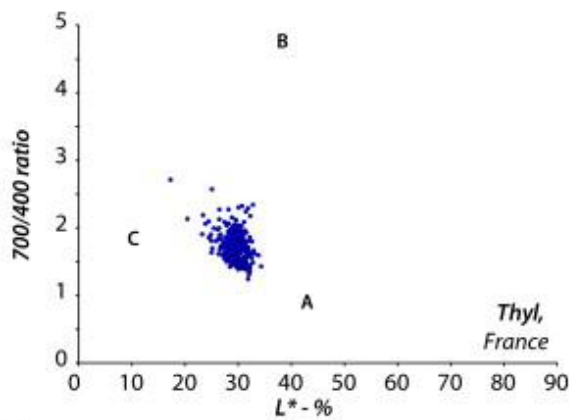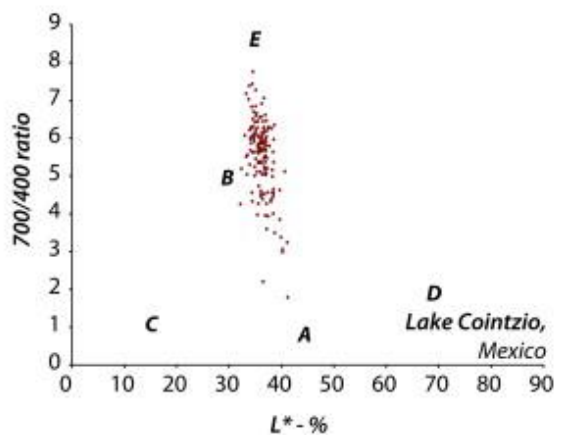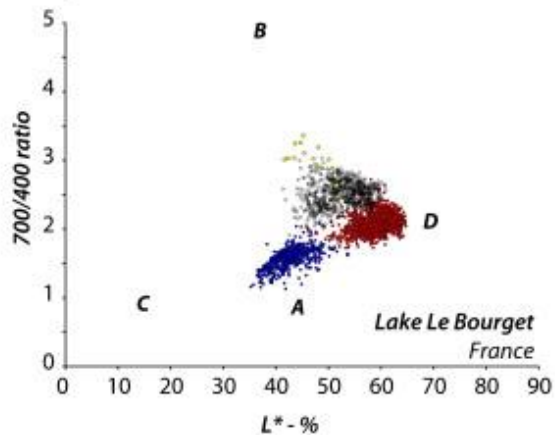
Fig. 4. : Q7/4 diagram: for palustrine environments with on the left, Thyl peat (Alps range, France) and on the right Chautagne peat (Alpine valley, France), for fjords environments, with on the left, Saanich Inlet (British Columbia, Canada) and on the right Corcovado fjord (Chile), for lacustrine environments, with on left Lake Le Bourget (Alpine Valley, France) and on the right Coïntzio Lake, Mexico.
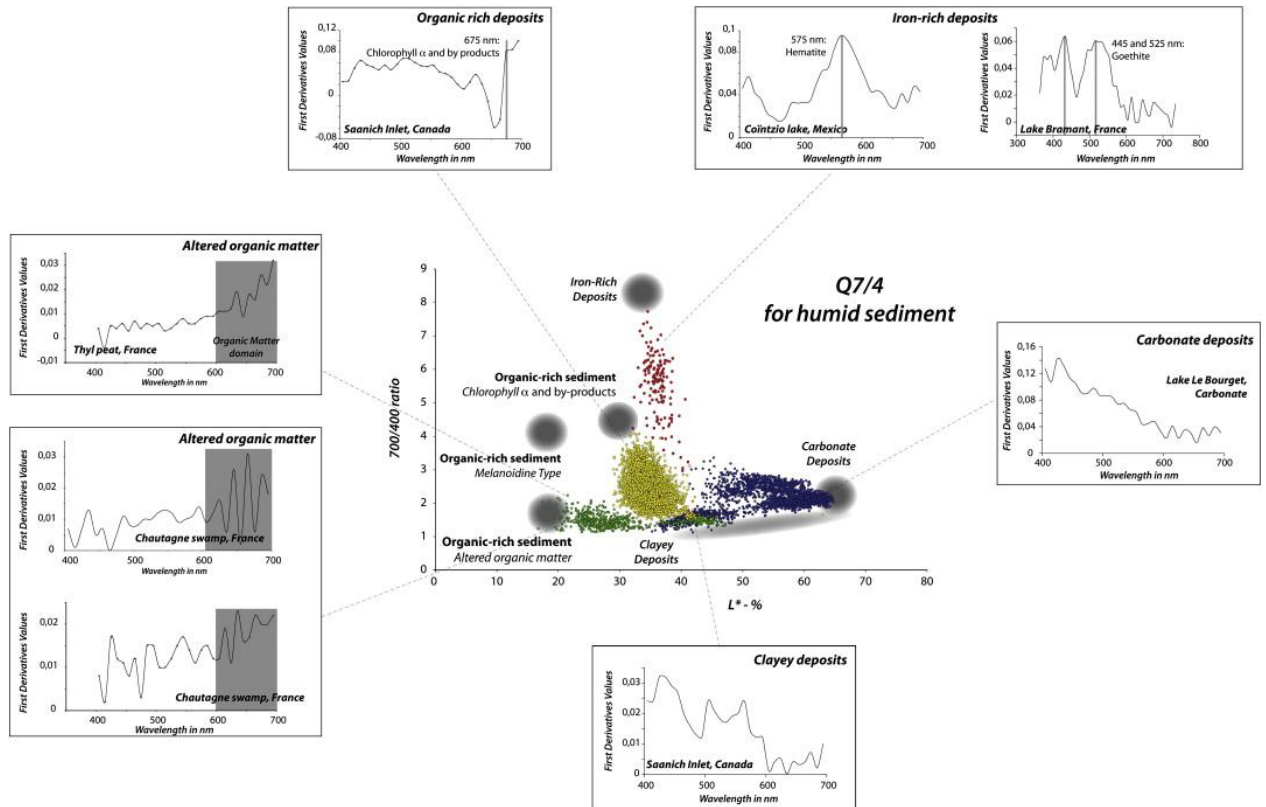
Fig. 5. : Q7/4 diagram for wet sediment combined with FDS allowed to distinguish 5 poles: clayey deposits, organic rich deposits (chlorophyll a and by products), altered organic matter deposits, iron rich deposits, and carbonated deposits. FDS analysis gives more details in the signature of some pole like for iron-rich deposits and altered organic matter pole.
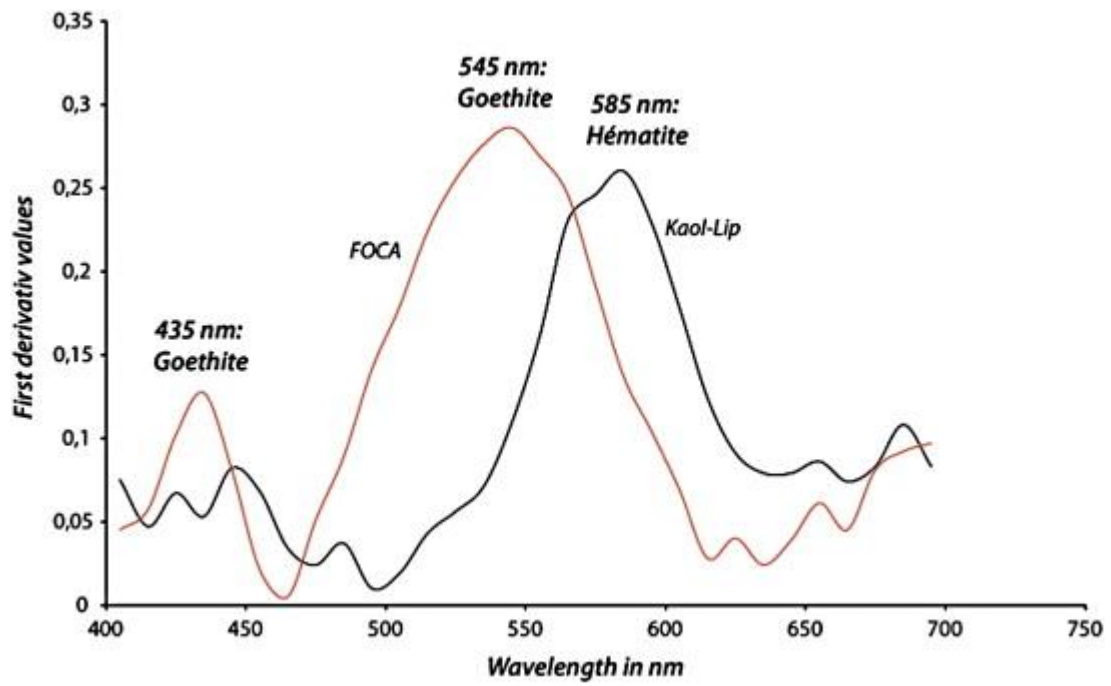
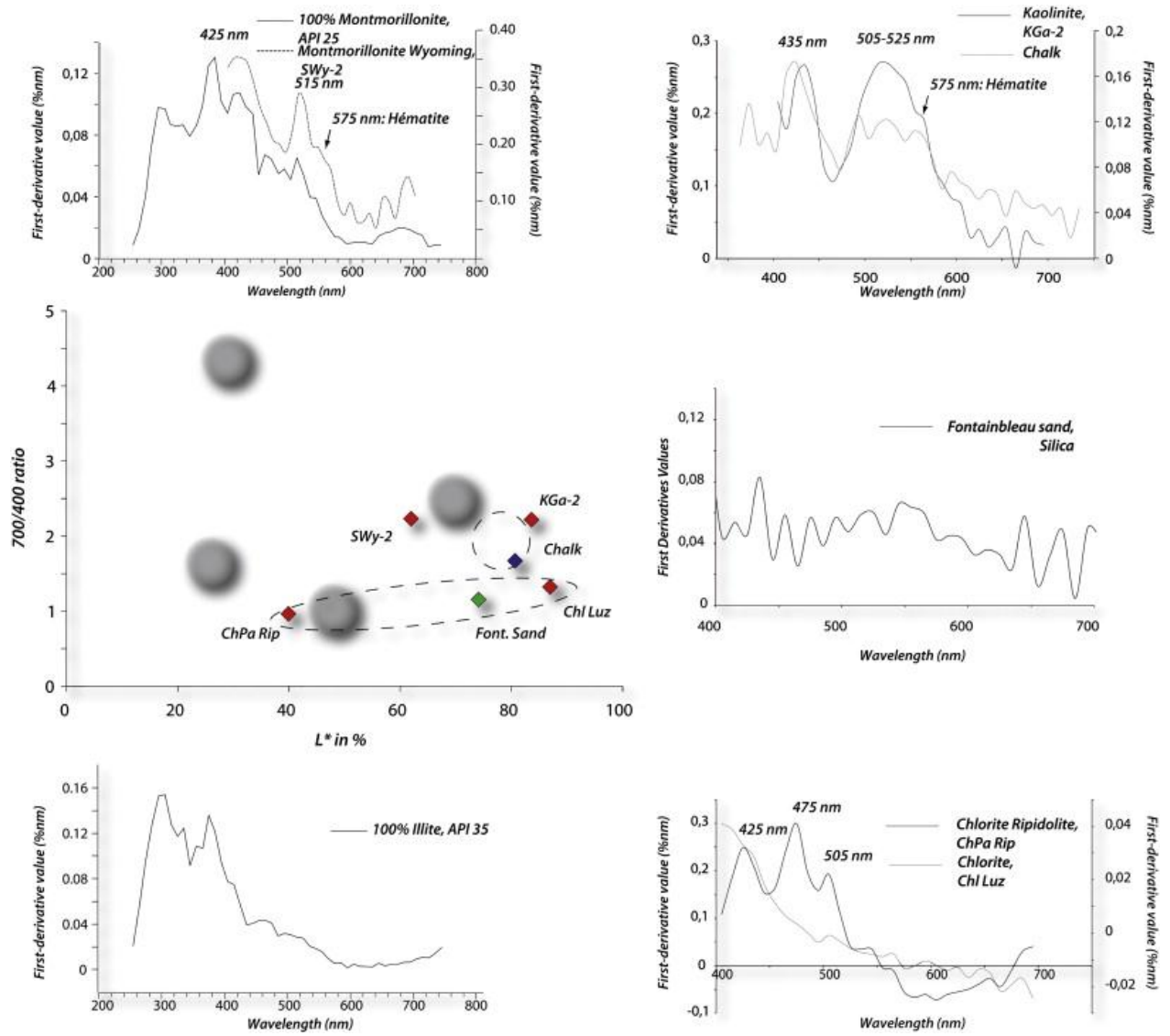Fig. 6. : Hematite FDS highlight a major peak around 585 nm whereas goethite can be recognized with the two peaks around 435 nm and 545 nm.

Fig. 7. : Position of chalk and clay standard samples in Q7/4 diagram.
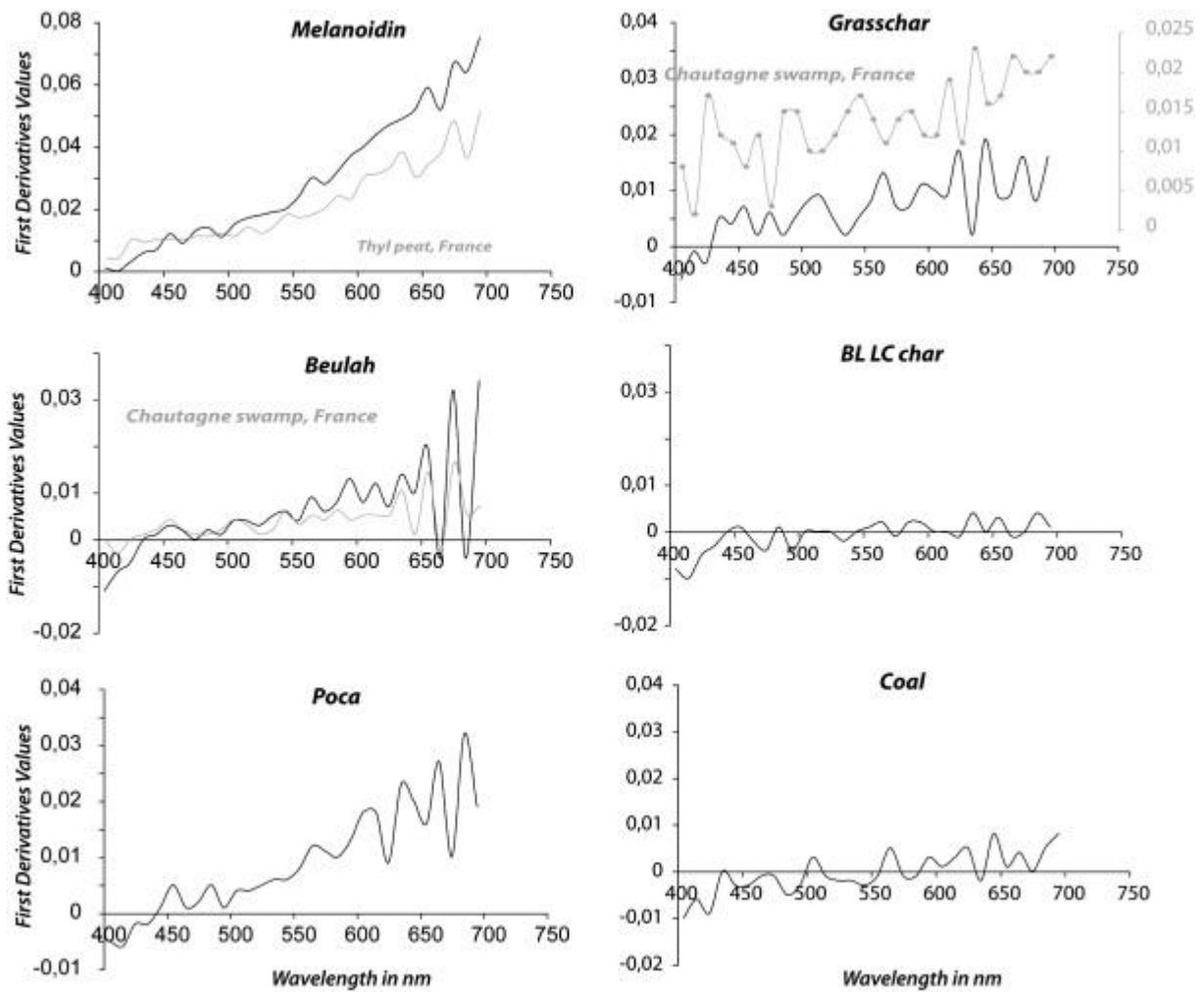
Fig. 8. : 3 international standards are compared with various samples from Chautagne and Thyl peat highlight various pattern that allowed distinguishing different types of organic matter. For the last 3 other standards, they were not observed in the various records however their analyses reinforced the usefulness of the tools because it is possible to differentiate coal, charcoal, soot, and black carbon in spite of a very low reflectance.
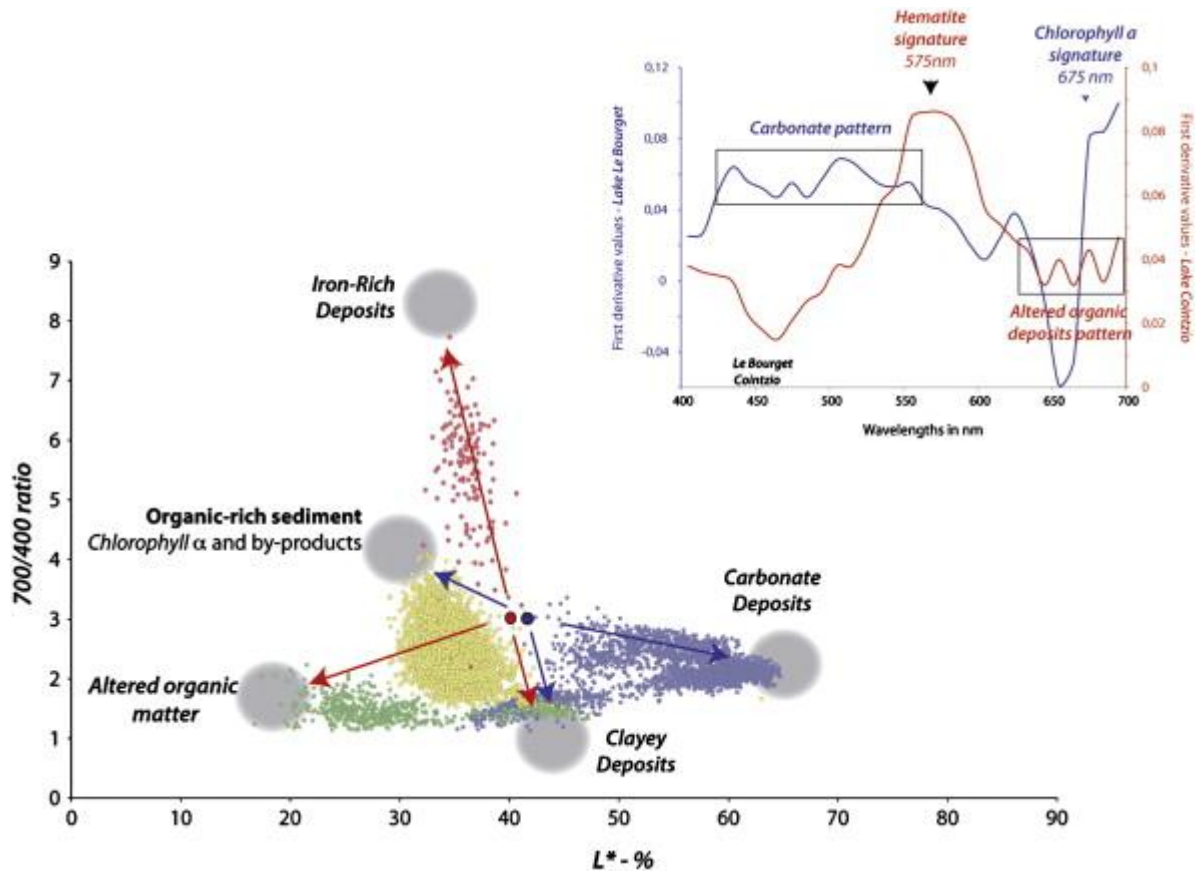
Fig. 9. : Two points, however, side by side, may carry different information. Effectively Cointzio Lake in red and Lake Le Bourget in blue suggest points close to each other. However, looking at the FDS (top right), the composition of the samples is clearly different with a 675 nm peak and a typical trend for carbonates Bourget cons a major peak in hématite and altered organic matter signal for Cointzio Lake. This example highlights the need to couple FDS and Q7/4 diagram to approach the analysis of sediment dynamics.
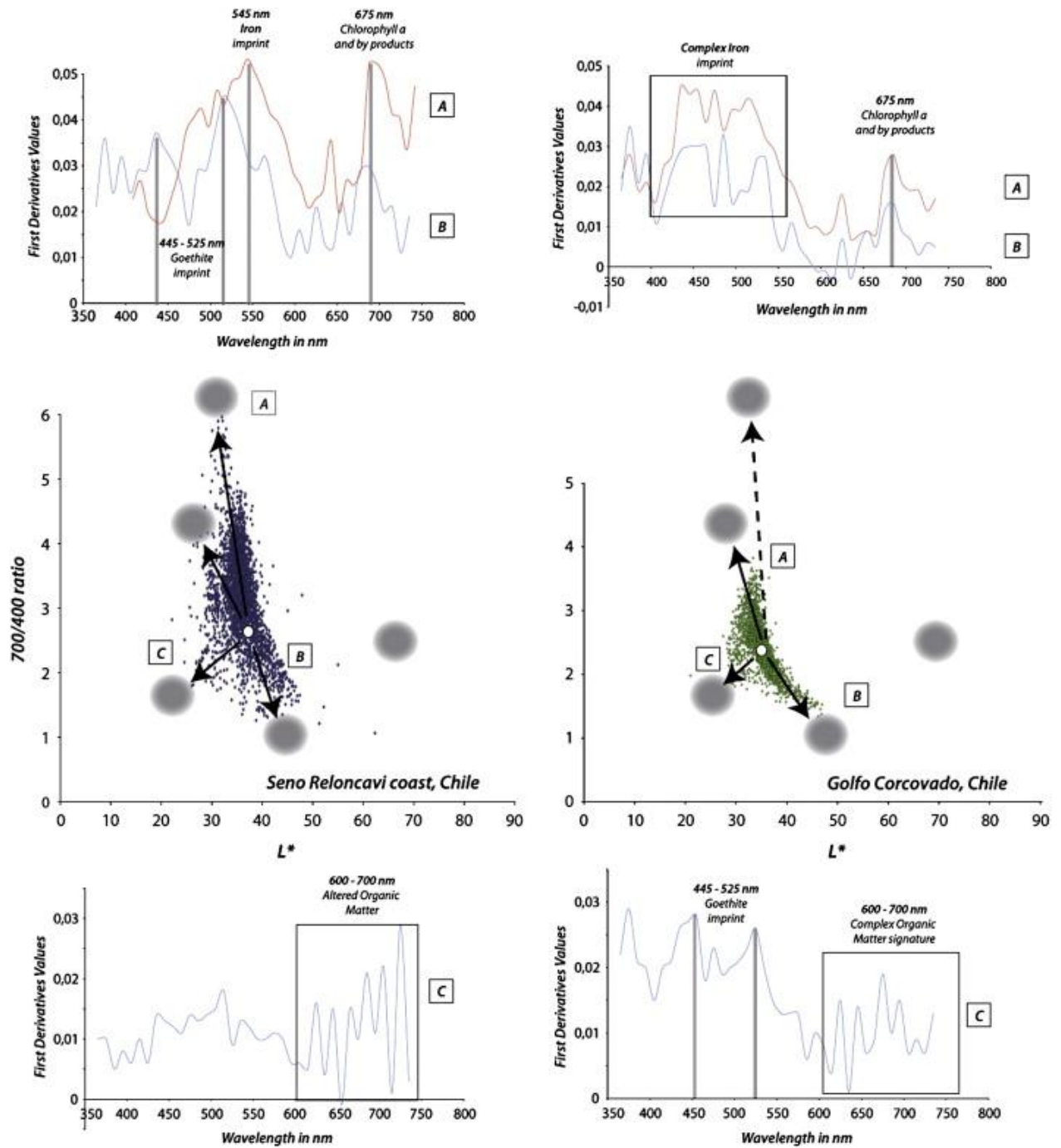
Fig. 10. : Illustration of the special care on the cloud point distributions when an apparent bipolarity is observed. FDS analysis reveals a much more complex system that implies 4 poles. On the left, the Reloncavi fjord indicates an organization around 4 poles as confirmed by FDS analysis (top and bottom). In the Corcovado Gulf, values seem rather organized around three major poles, the iron rich deposition pole being less present.
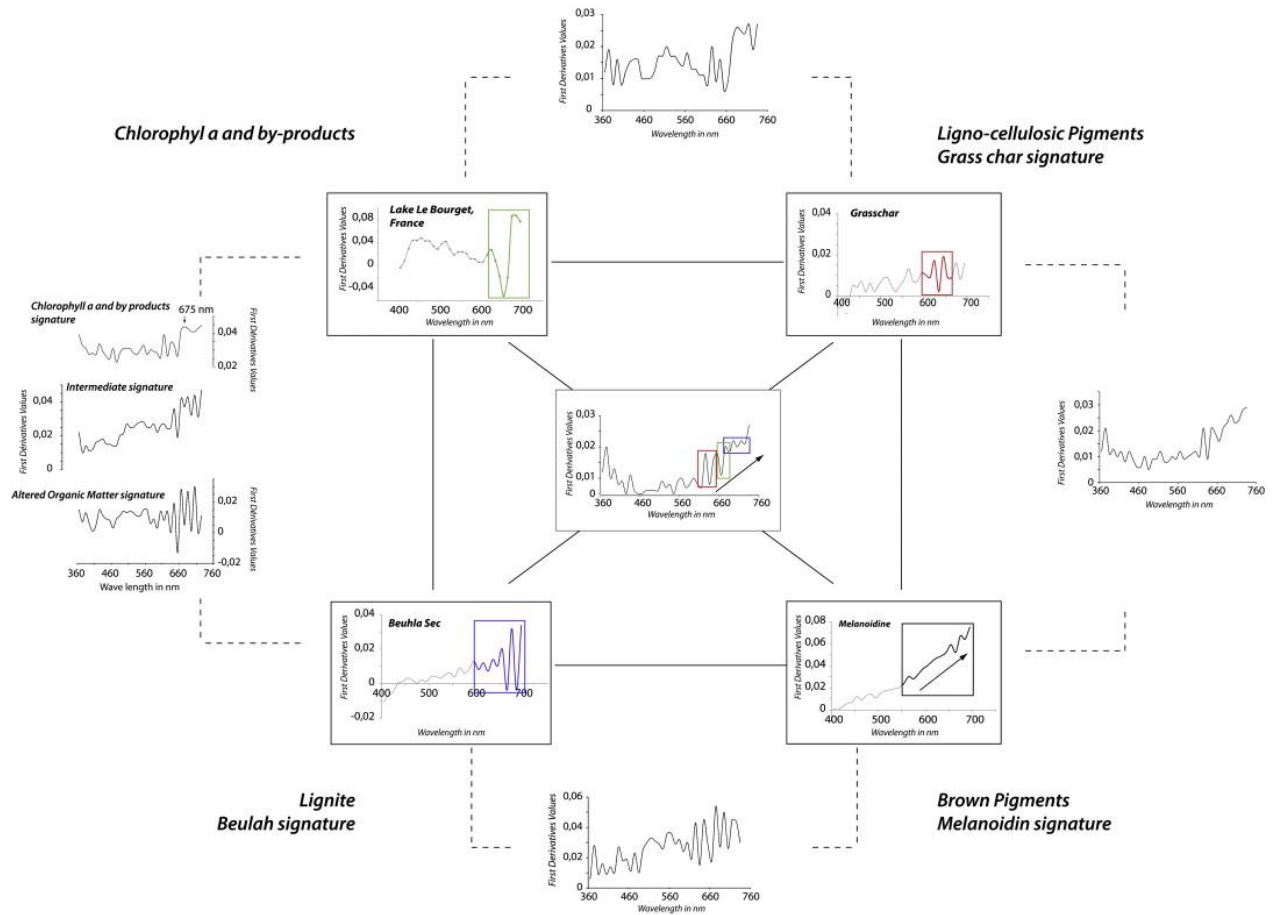
Fig. 11. : Block diagram illustrating the superposition of different FDS from fresh and altered organic matter in sediments from Lake Ossa. The 4 corners of the square correspond to differing states of organic matter as expressed in FDS: the pigments of chlorophyll a and melanoidin, the ligniocellulosic compounds (Grass char) and lignite (Beuhla).